NASA Technical Memorandum 101528

A REVIEW OF REACTION RATES AND THERMODYNAMIC AND TRANSPORT PROPERTIES FOR THE 11-SPECIES AIR MODEL FOR CHEMICAL AND THERMAL NONEQUILIBRIUM CALCULATIONS TO 30000 K

(NASA-TM-101528) A REVIEW OF REACTION RATES AND THERMODYNAMIC AND TRANSPORT PROPERTIES FOR THE 11-SPECIES AIR MODEL FOR CHEMICAL AND THERMAL NONEQUILIBRIUM CALCULATIONS TO 30000 K (NASA) 69 p CSCL 20D G3/34

N89-21193

Unclas
0197256

Roop N. Gupta

Jerrold M. Yos

Richard A. Thompson

February 1989

National Aeronautics and
Space Administration

Langley Research Center
Hampton, Virginia 23665-5225

Summary

Reaction rate coefficients and thermodynamic and transport properties are provided for the 11-species air model which can be used for analyzing flows in chemical and thermal nonequilibrium. Such flows will likely occur around currently planned and future hypersonic vehicles. Guidelines for determining the state of the surrounding environment are provided. Approximate and more exact formulas are provided for computing the properties of partially ionized air mixtures in such environments.

Introduction

Currently envisaged transatmospheric and aeroassist missions (refs. 1,2,3, and 4) have created a resurgence of interest in the aerothermodynamic design of hypersonic vehicles. However, the velocities and altitudes at which these proposed craft would operate are different, and sometimes more severe, than have been experienced in the past. As a result, the nonequilibrium flow environment which will surround these vehicles will considerably impact the vehicle aerodynamics, thermal loads, and propulsion system efficiency. Since such an environment is difficult to simulate in current ground based-test facilities, the design of these future vehicles will rely heavily on numeric calculations. In turn, these calculations will require a good understanding of the physical modelling required to simulate these phenomena.

Under hypersonic flight conditions, a vehicle travelling through the atmosphere will excite the air which flows around the body to very high temperatures as kinetic energy from the vehicle is transferred. Depending on the flight velocity, various chemical reactions will be produced behind a shock wave as shown in figure 1 (which is adapted from ref. 5) for the stagnation region of a 30.5 *cm* (1 ft) radius sphere. These reactions will affect the properties of air and cause considerable deviation from those of a thermally and calorifically perfect gas. A vehicle flying through the higher reaches of the atmosphere at high velocities may also experience thermal nonequilibrium (fig. 1), since the lower density reduces the collision frequency, and the high velocity results in smaller transit times for the air molecules. Both of these processes create a delay in the equilibration of translational, rotational and vibrational modes of the thermal energy. Under these conditions, the modelling of the air chemistry requires a multi-temperature approach in contrast to classical single temperature formulations.

Figure 1 delineates four regions (I through IV), showing when the various chemical activities are initiated at a given altitude and velocity. Similarly, it also depicts through Regions A, B and C the initiation of chemical and thermal nonequilibrium processes for different velocity and altitude conditions. This figure clearly shows that the reaction rate coefficients and thermodynamic and transport properties would change continuously for a given flight trajectory. For example, in regions A and B (i.e., before initiation of thermal nonequilibrium), the specific heat at constant pressure C_p would change as follows:

C_p = constant in Region I, before the excitation of vibrational energy mode

= $C_p(T)$ in Region I, after the excitation of vibrational energy mode and before the dissociation of oxygen

= $C_p(C_i,T)$ after the dissociation of oxygen

Similarly, the equation of state would change along the flight trajectory as the thermal equilibrium and thermal nonequilibrium regions (ref. 6) are traversed.

$$p = \rho \frac{R_{univ}}{\overline{M}} T \quad \text{in Regions A and B}$$

$$= \rho \frac{R_{univ}}{\overline{M}} T_{tr} \quad \text{in Region C}$$

In numerical simulations, the thermodynamic and transport properties and reaction rate coefficients (in the case of finite rate chemistry) are typically required. It is obvious from the previous discussion that these properties and the equation of state should be evaluated carefully when chemical and thermal nonequilibrium conditions exist in the flowfield around a hypersonic vehicle. Under chemical and thermal equilibrium conditions, the transport and thermodynamic properties of high temperature air and its components are well documented in the literature (refs. 7,8, and 9). However, for flows with finite-rate chemistry the individual species properties and appropriate mixing laws which are required are not as well established. For example, in a partially ionized gas mixture, the conventional mixing laws (refs. 10 and 11) developed for non-ionized mixtures can not be extended to higher temperatures without considerable error (ref. 12).

The purpose of this report is to provide thermodynamic and transport properties and the reaction rate coefficients of the most important reactions for the 11 constituent species of air ($N, O, N_2, O_2, NO, N^+, O^+, N_2^+, O_2^+, NO^+, e^-$) for temperatures up to 30000 K. Approximate and more exact mixing laws are also provided for partially ionized gas mixtures. Sources of the input data used in the calculation of various flowfield properties are identified. Appropriate formulas are provided for using these properties in computations of flows with thermal nonequilibrium.

Symbols

A_n	coefficients of polynomial curve-fits for thermodynamic properties, $n = 1,2...,7$
$A_{b,r}$	coefficient in the Arrhenius form of backward reaction rate constant
$A_{f,r}$	coefficient in the Arrhenius form of forward reaction rate constant
A_{ij}	nondiagonal matrix elements of the first Chapman-Enskog formula
A_{ij}^*	ratio of collision cross sections, $\overline{\Omega}_{ij}^{(2,2)} / \overline{\Omega}_{ij}^{(1,1)}$
$A_{\overline{D}_{ij}}$, $B_{\overline{D}_{ij}}$, $C_{\overline{D}_{ij}}$, $D_{\overline{D}_{ij}}$	curve-fit coefficients for diffusion coefficient $\overline{D}_{ij}$
$A_{K_{f,i}}$, $B_{K_{f,i}}$, $C_{K_{f,i}} D_{K_{f,i}}$, $E_{K_{f,i}}$	coefficients of polynomial curve fits for frozen thermal conductivity of species i
A_{μ_i}, B_{μ_i}, C_{μ_i}, D_{μ_i}, E_{μ_i}	curve-fit coefficients for viscosity of species i
$A_{\overline{\Omega}_{ij}^{(1,1)}}$, $B_{\overline{\Omega}_{ij}^{(1,1)}}$, $C_{\overline{\Omega}_{ij}^{(1,1)}}$, $D_{\overline{\Omega}_{ij}^{(1,1)}}$	curve-fit coefficients for collision cross section $\overline{\Omega}_{ij}^{(1,1)}$

$A_{\overline{\Omega}_{ij}^{(2,2)}}$, $B_{\overline{\Omega}_{ij}^{(2,2)}}$, $C_{\overline{\Omega}_{ij}^{(2,2)}}$, $D_{\overline{\Omega}_{ij}^{(2,2)}}$ curve-fit coefficients for collision cross section $\overline{\Omega}_{ij}^{(2,2)}$

$A_{B_{ij}^*}$, $B_{B_{ij}^*}$, $C_{B_{ij}^*}$, $D_{B_{ij}^*}$ curve-fit coefficients for collision cross section ratio B_{ij}^*

B_{ij}^* ratio of collision cross sections, $(5\overline{\Omega}_{ij}^{(1,2)} - 4\overline{\Omega}_{ij}^{(1,3)})/\overline{\Omega}_{ij}^{(1,1)}$

$B_{b,r}$ temperature exponent for backward reaction rate constant

$B_{f,r}$ temperature exponent for forward reaction rate constant

C_i mass fraction of species i

C_p specific heat at constant pressure, $\left[\frac{\partial h}{\partial T}\right]_p$, $cal/gm-mole-K$

C_{p_d} diffusion specific heat at constant pressure, $\left[\sum_{i=1}^{NS} h_i \frac{\partial C_i}{\partial T}\right]_p$, $cal/gm-mole-K$

C_{p_f} frozen specific heat, $C_{p_f} = \sum_{i=1}^{NS} C_i C_{p,i} = \left[\frac{\partial h}{\partial T} - \sum_{i=1}^{NS} h_i \frac{\partial C_i}{\partial T}\right]_p$, $cal/gm-mole-K$

$C_{p,i}$ specific heat of species i, $\left[\frac{\partial h_i}{\partial T}\right]_p$, $cal/gm-mole-K$

D_{ii} coefficient of self-diffusion, cm^2/sec

D_{ij} binary diffusion coefficient, cm^2/sec

$E_{b,r}$ activation energy for the backward reaction r, $erg/gm-mole$

$E_{f,r}$ activation energy for the forward reaction r, $erg/gm-mole$

F_i^o free energy of species i at 1 atm pressure (standard state), $cal/gm-mole$

h enthalpy of mixture, $\sum_{i=1}^{NS} C_i h_i$, $cal/gm-mole$

h_i enthalpy of species i, $cal/gm-mole$

$h_{i,vib}$ vibrational component of enthalpy of a molecular species i, $cal/gm-mole$

$(\Delta h_i^f)_{T_{ref}}$ standard heat of formation of species i at temperature T_{ref}, $cal/gm-mole$

J_i^k diffusion mass flux of species i, gm/cm^2-sec

K total effective thermal conductivity of mixture in thermodynamic equilibrium, $K_f + K_d$ *or* $K_f + K_r$, $cal/cm-sec-K$

K_d diffusion component of thermal conductivity of mixture defined by equation (A14), $cal/cm-sec-K$

K_e thermal conductivity of electrons, $cal/cm-sec-K$

K_e' thermal conductivity of electrons due to electron-electron collisions only, $cal/cm-sec-K$

K_{el} component of thermal conductivity of mixture due to electron excitation, $cal/cm-sec-K$

K_f	frozen thermal conductivity of mixture in thermodynamic equilibrium, $K_{tr} + K_{int}$, $cal/cm-sec-K$
$K_{f,i}$	frozen thermal conductivity of species i in thermodynamic equilibrium, $K_{tr,i} + K_{int,i}$, $cal/cm-sec-K$
K_{int}	internal component of frozen thermal conductivity of a mixture in thermodynamic equilibrium, $K_{rot} + K_{vib} + K_{el}$, $cal/cm-sec-K$
$K_{int,i}$	internal component of the frozen thermal conductivity of species i in thermodynamic equilibrium, $cal/cm-sec-K$
K_r	reaction component of thermal conductivity of mixture defined by equation (A16), $cal/cm-sec-K$
$K_{tr}, K_{tr}^{(1)}$	translational thermal conductivity of mixture from first Chapman-Enskog approximation, $cal/cm-sec-K$
K_{tr}^{*}	translational thermal conductivity of mixture without contributions due to electron-heavy particle collisions, $K_{tr} - K_e$, $cal/cm-sec-K$
$K_{tr,i}$	translational component of thermal conductivity of species i, $cal/cm-sec-K$
K_{vib}	vibrational component of thermal conductivity of mixture, $cal/cm-sec-K$
k	Boltzmann's constant, 1.38×10^{-16} erg/K
$k_{b,r}$	backward reaction rate coefficient for reaction r, $cm^3/mole-sec$ or $cm^6/mole^2-sec$
$k_{f,r}$	forward reaction rate coefficient for reaction r, $cm^3/mole-sec$
$Le_{f,i}$	frozen binary Lewis number, $\rho C_{p_f} D_{ij}/K_f$
$Le_{r,i}$	reactive binary Lewis number, $\rho C_p D_{ij}/K$
M_i	molecular weight of species i, $gm/gm-mole$
M	molecular weight of mixture, $gm/gm-mole$
N_A	Avogadro's number, 6.0225×10^{23} $molecules/gm-mole$
n	number density, $particles/cm^3$
Pr_f	frozen Prandtl number, $C_{p_f}\mu/K_f$
Pr_r	reactive Prandtl number, $C_p\mu/K$
p	pressure, $dyne/cm^2$
q^k	kth component of the overall heat flux vector, cal/cm^2-sec
q_e^k	kth component of the electron heat flux vector due to electron-electron collisions, cal/cm^2-sec
q_{vib}^k	kth component of the vibrational heat flux vector due to molecule-molecule collisions, cal/cm^2-sec
R_{univ}	universal gas constant, 1.987 $cal/gm-mole-K$
T	temperature under thermodynamic equilibrium, K
$T_{D_{b,r}}$	characteristic reaction temperature for the backward reaction r, $E_{b,r}/k$, K

$T_{D_{f,r}}$	characteristic reaction temperature for the forward reaction r, $E_{f,r}/k$, K
T_e	electron temperature, K
T_{el}	electronic excitation temperature, K
T_{ref}	reference temperature, 298.15 K
T_{rot}	rotational temperature, K
T_{tr}	translational temperature, K
T_{ve}	vibrational-electron-electronic excitation temperature, K
T_{vib}	vibrational temperature, K
t	time, sec
V_i^k	kth component of diffusion velocity of species i, cm/sec
$\dot{w}_i$	mass rate of formation of species i, g/cm^3-sec
X_i	concentration of species i, $moles/volume$
x^k	kth component of general orthogonal coordinate system
x_i	mole-fraction of species i
$\alpha_{i,r}$	stoichiometric coefficients for reactants
$\beta_{i,r}$	stoichiometric coefficients for products
γ_j	mole mass ratio of species j, X_j/ρ
$\mu^{(1)}, \mu$	viscosity of mixture from first Chapman-Enskog approximation, $gm/cm-sec$
μ_i	viscosity of species i, $gm/cm-sec$
ρ	density of the mixture, gm/cm^3
ρ_i	density of species i, gm/cm^3
$\overline{\Omega}_{ij}^{(1,1)}$	average collision cross section (for diffusion, viscosity, and translational, internal and reaction components of thermal conductivity) for collisions between the species i and j, Å^2; $1\ \text{Å} = 10^{-8} cm$
$\overline{\Omega}_{ij}^{(2,2)}$	average collision cross section (for viscosity and translational component of thermal conductivity) for collisions between the species i and j, Å^2
$\overline{\Omega}_{ij}^{(1,2)}, \overline{\Omega}_{ij}^{(1,3)}$	average collision cross sections (for translational component of thermal conductivity) for collisions between the species i and j, Å^2

Subscripts:

b	backward reaction
e	electron
el	electronic excitation
f	forward reaction
i	species i

j	species j
p	constant pressure
r	rth reaction
ref	reference condition
rot	rotational energy mode
tr	translational energy mode
ve	vibrational-electron-electronic energy mode
v	total number of species, $\equiv NS$

Abbreviations:

AOTV	Aeroassisted Orbital Transfer Vehicle
NASP	National Aero-Space Plane
NIR	total number of independent reaction
NJ	sum of the reacting species (NS) plus the number of catalytic bodies
NR	total number of reactions
NS	total number of species

Chemical Kinetic Model and Reaction Rates

When chemical reactions proceed at a finite rate, the rate of production terms appear in the energy equation when formulated in terms of temperature and in the species continuity equations (refs. 13,14,15). For a multicomponent gas with NS reacting chemical species and NR chemical reactions, the stoichiometric relations for the overall change from reactants to products are:

$$\sum_{i=1}^{NJ} \alpha_{i,r} X_i \underset{k_{b,r}}{\overset{k_{f,r}}{\rightleftarrows}} \sum_{i=1}^{NJ} \beta_{i,r} X_i \tag{1}$$

where $r=1,2,...,NR$ and NJ is equal to the sum of the reacting species (NS) plus the number of catalytic bodies. The quantities $\alpha_{i,r}$ and $\beta_{i,r}$ are the stoichiometric coefficients for reactants and products, respectively, and $k_{f,r}$ and $k_{b,r}$ are the forward and backward rate constants. The quantities X_i denote the concentrations of the chemical species and catalytic bodies in moles per unit volume. The catalytic bodies ($NJ-NS$) may be chemical species or linear combinations of species that do not undergo a chemical change during the reaction.

The net mass rate of production of the ith species per unit volume resulting from all the reactions NR may be obtained (ref. 14) from

$$\dot{w}_i = M_i \sum_{r=1}^{NR} \left[\frac{dX_i}{dt} \right]_r = \sum_{r=1}^{NR} \left[\frac{d\rho_i}{dt} \right]_r \tag{2a}$$

or

$$\dot{w}_i = M_i \sum_{r=1}^{NR} (\beta_{i,r} - \alpha_{i,r})(R_{f,r} - R_{b,r}) \tag{2b}$$

where

$$R_{f,r} = k_{f,r} \prod_{j=1}^{NJ} (\gamma_j \rho)^{\alpha_{j,r}} \tag{2c}$$

$$R_{b,r} = k_{b,r} \prod_{j=1}^{NJ} (\gamma_j \rho)^{\beta_{j,r}} \tag{2d}$$

Here, the mole-mass ratio γ_j is defined as

$$\gamma_j = \begin{cases} \dfrac{X_j}{\rho} = \dfrac{C_j}{M_j} & j = 1,2,\ldots,NS \\ \displaystyle\sum_{i=1}^{NS} Z_{(j-NS),i}\, \gamma_i & j = NS+1,\ldots,NJ \end{cases} \tag{2e}$$

The constants $Z_{(j-NS),i}$ are determined from linear dependence of the catalytic bodies upon the NS species. Values of these constants for the 11-species air model are given in table I.

The reaction rates in equation (1) or equations (2c) and (2d) are expressed in the Arrhenius form as:

$$k_{f,r} = A_{f,r} T^{B_{f,r}} \exp(-T_{D_{f,r}}/T) \ , \quad \frac{1}{s}\left[\frac{mole}{cm^3}\right]^{-\alpha_r} \tag{3a}$$

$$k_{b,r} = A_{b,r} T^{B_{b,r}} \exp(-T_{D_{b,r}}/T) \ , \quad \frac{1}{s}\left[\frac{mole}{cm^3}\right]^{-\beta_r} \tag{3b}$$

where

$$\alpha_r = \sum_{i=1}^{NJ} \alpha_{i,r} - 1 \tag{4a}$$

$$\beta_r = \sum_{i=1}^{NJ} \beta_{i,r} - 1 \tag{4b}$$

and $T_{D_{f,r}}$ and $T_{D_{b,r}}$ are the characteristic reaction temperatures for the forward and backward reactions, respectively. Values for the reaction rates $k_{f,r}$ and $k_{b,r}$ are tabulated in table II for the 11-species air model. For a specified temperature, density, and species composition, equations (2) through (4) can be used to obtain the production rate of a species i in a multicomponent gas by employing the catalytic body efficiencies and reaction rates from tables I and II. The first seven reactions and reaction rates in table II are taken from reference 16 and were employed in reference 13 for the 7-species air model ($N, O, N_2, O_2, NO, NO^+, e^-$). Reaction rates for reactions 8 through 20 of table II are taken from reference 17. Some of these reactions have been regrouped here (and in ref. 18) through the use of third bodies M_1 through M_4 which is similar to the approach in reference 13.

The reaction rates given in table II were originally used by Blottner (ref. 13) and Dunn and Kang (ref. 17) in the context of a single temperature assuming thermal equilibrium. One may use Park's (ref. 19) guidelines (in the context of his two-temperature model) for defining the rate controlling temperature in dissociation and electron impact ionization reactions under thermal nonequilibrium conditions. This was done in reference 20, for example.

Park has suggested the use of a temperature weighted with the vibrational temperature to characterize dissociation reactions, based on the preferential dissociation concept. The reaction rates in Park's model are assumed to be dictated by the geometric average temperature

$$T_{av} = \sqrt{T_{tr} T_{vib}} \tag{5}$$

and the dissociation reaction rates are given by

$$k_{f,r} = A_{f,r} T_{av}^{B_{f,r}} \exp(-T_{D_{f,r}}/T_{av}) \tag{6}$$

Treanor and Marrone (refs. 21 and 22) have suggested a more rational (but slightly more difficult) way than Park's to account for the effect of vibrational relaxation on dissociative reactions with the preferential dissociation concept. They have suggested the use of a vibrational coupling factor (refs. 20,21, and 22) with the dissociation reaction rates obtained under the assumption of thermal equilibrium.

Recent work of Jaffe (ref. 23), based on collision theory and using methods of statistical mechanics, found no evidence of preferential weighting to any particular energy mode in obtaining the total energy available in a collision whether it is an elastic, inelastic, or reactive encounter. Jaffe found that the multi-temperature effects on the reaction rates were small for dissociation. These findings were supported by those of Moss et al. (ref. 24), who carried out flowfield analyses employing the Direct Simulation Monte Carlo (DSMC) approach. Thus, a weaker dependence of $k_{f,r}$ on T_{vib} (such as the one recently suggested by Sharma et al. (ref. 25) as $T_{av} = T_{tr}^{0.7} T_{vib}^{0.3}$) might be more realistic, especially for highly energetic flows.

It is obvious that the multi-temperature kinetic models for high energy flows based on both preferential and non-preferential dissociation assumptions employ some degree of empiricism. They exemplify the degree of uncertainty which exists in modelling the multi-temperature kinetics. Quantum mechanical studies of the type in reference 23 supplemented by non-obtrusive laser diagnostic studies would be desirable to establish these models on a sounder basis.

Species Thermodynamic Properties and Mixture Formulas

Thermodynamic properties (i.e., $C_{p,i}$ and h_i) are required for each species considered in a finite-rate flowfield calculation. For calculations with chemical equilibrium, the free energies F_i are also required. Since the multicomponent gas mixtures are considered to be mixtures of thermally perfect gases, the thermodynamic properties for each species are calculated by using the local static temperature. Then, properties for the gas mixture are determined in terms of the individual species properties through the relations:

$$h = \sum_{i=1}^{NS} C_i h_i \tag{7a}$$

with

$$h_i = \int_{298}^{T} C_{p,i} dT + (\Delta h_i^f)_{T=298\,K} \tag{7b}$$

and

$$C_{p_f} = \sum_{i=1}^{NS} C_i C_{p,i} \tag{8a}$$

with

$$C_{p,i} = \left[\frac{\partial h_i}{\partial T}\right]_p \tag{8b}$$

Note that C_{p_f} for a mixture defined through equation (8a) is the 'frozen' specific heat. This definition does not account for species production or conversion due to chemical reactions. Frozen specific heat is commonly employed in defining the Prandtl and Lewis numbers† for a mixture and is related to the mixture enthalpy h through the relation

$$C_{p_f} = \left[\frac{\partial h}{\partial T} - \sum_{i=1}^{NS} h_i \frac{\partial C_i}{\partial T}\right]_p = \sum_{i=1}^{NS} C_i C_{p,i} \tag{9}$$

Expressions for $C_{p,i}$ using the partition function approach were obtained in reference 26, whereas references 27 and 28 employed a virial coefficient method. The partition function formulation is quite accurate at low temperatures; however, this formulation becomes less accurate at high temperatures because of the introduction of errors from several sources such as non-rigidity of the rotor and anharmonicity of the oscillator. The virial formulation defines the potential-energy surface more accurately at higher temperatures in comparison with the partition function approach. Using the virial formulation, Browne (refs. 27 and 28) obtained the thermodynamic properties as corrections to those of the monatomic gas in terms of the first and second virial coefficients and their temperature derivatives. These data can be used to separate the contributions of different internal energy modes to the specific heat as is required in the case of multi-temperature flowfield models. For example, in a two-temperature model (refs. 19 and 20), advantage may be taken of the fact that the translational and rotational energy modes are fully excited at room temperature, and therefore, the heat capacities for these modes are independent of temperature. The combined vibrational-electronic specific heat for species i, $(C_{p,i})_{ve}$, can then be evaluated by using the value for the total specific heat, $C_{p,i}$, evaluated at temperature T_{ve} and subtracting out the constant contribution from the translational and rotational specific heats. This can be described (see fig. 2 for the various contributions) by

$$[(C_{p,i})_{ve}]_{T_{ve}} = [C_{p,i}]_{T_{ve}} - (C_{p,i})_{tr} - (C_{p,i})_{rot} \tag{10}$$

The enthalpy, h_i, for a two-temperature model can be evaluated similarly, since contributions from the translational and rotational modes are linear with temperature. Therefore, the vibrational-electronic enthalpy for species i, $(h_i)_{ve}$, can be obtained from the specific enthalpy h_i evaluated at temperature T_{ve} and subtracting out the contribution from the translational and rotational enthalpies evaluated at T_{ve} as well as the enthalpy of formation.

$$[(h_i)_{ve}]_{T_{ve}} = [h_i]_{T_{ve}} - [(C_{p,i})_{tr} + (C_{p,i})_{rot}](T_{ve} - T_{ref}) - (\Delta h_i^{\,f})_{T_{ref}} \tag{11}$$

† See Appendix A for the various definitions.

The specific enthalpy from all the contributions of internal energy modes can then be obtained by adding the contributions of translational and rotational enthalpies (evaluated at the translational-rotational temperature) and the enthalpy of formation to the vibrational-electronic enthalpy as follows

$$h_i(T,T_{ve}) = [(h_i)_{ve}]_{T_{ve}} + [(C_{p,i})_{tr}+(C_{p,i})_{rot}](T-T_{ref}) + (\Delta h_i^f)_{T_{ref}} \qquad (12)$$

Reference 26 has provided curve fits for $C_{p,i}$ and h_i, whereas references 27 and 28 have provided tabulations of these data. Since the use of curve fits reduces the expense of computing the original functional relations, these thermodynamic properties have been curve fitted here as a function of temperature for the temperature range of 300 K $\leq T \leq$ 30000 K. These curve fits include those of reference 26 for the range 300 K $\leq T \leq$ 6000 K, and new curve fits are provided to the tabulated values of references 27 and 28 for the range 6000 K $\leq T \leq$ 30000 K. The following polynomial equations are employed for these curve fits:

Specific heat:

$$\frac{C_{p,i}}{R_{univ}} = A_1 + A_2T + A_3T^2 + A_4T^3 + A_5T^4 \qquad (13)$$

Specific enthalpy:

$$\frac{h_i}{R_{univ}T} = A_1 + \frac{A_2T}{2} + \frac{A_3T^2}{3} + \frac{A_4T^3}{4} + \frac{A_5T^4}{5} + \frac{A_6}{7} \qquad (14)$$

For equilibrium calculations, the following curve fit for the free energies F_i may be used:

$$\frac{F^{o_i}}{R_{univ}T} = A_1[1-ln(T)] - \frac{A_2T}{2} - \frac{A_3T^2}{6} - \frac{A_4T^3}{12} - \frac{A_5T^4}{20} + \frac{A_6 - A_7}{T} \qquad (15)$$

where F^{o_i} is the free energy of species i at 1 *atm* pressure (standard state).

A tabulation of the polynomial constants (A_1 to A_7) for the 11-species air model is given in table III. A least squares technique has been used for obtaining the polynomial coefficients for the five temperature ranges between 300 and 30000 K. To assure a smooth variation of thermodynamic properties over the entire temperature range, values of A_1 to A_7 should be linearly averaged across the curve-fit boundaries (i.e., 800< T < 1200, 5500< T < 6500, 14500< T < 15500, and 24500< T < 25500). An example subroutine which evaluates the polynomial curve fits and performs the linear averaging is presented in appendix B. This routine may be easily modified to suit the user's requirements.

It may be mentioned here that temperature, T, in equations (13) through (15) is in $°K$. With the universal gas constant in $cal/gm-mole-K$, the specific heat and enthalpies will have the units of $cal/gm-mole-K$ and $cal/gm-mole$ respectively. The constant A_6 in these equations is related to the heat of formation through the relation

$$A_6R_{univ} = (\Delta h_i^f)_{T=298\,K} \qquad (16)$$

Figure 3 compares the values of specific heat obtained from the polynomial curve fit (eq. (13)) with the data of McBride et al. (ref. 26) and Browne (ref. 28). Values provided by Hansen (ref. 29) are also included for comparison. Hansen's values begin to deviate from those of references 26 and 28 beyond 4000 K for O_2 (fig. 3(a)), beyond 8000 K for N_2 (fig. 3(b)), and beyond 6000 K for NO (fig. 3(c)). This may

be due to the rigid-rotator and harmonic-oscillator partition function employed by Hansen. At higher temperatures, the population of levels corresponding to the non-parabolic regions of the potential energy curve are no longer negligible, and it becomes necessary to introduce the non-rigidity and anharmonicity corrections into the energy levels of the molecules as was done in reference 28.

Species Transport Properties and Mixture Formulas

The transport properties required in flowfield calculations are viscosity, thermal conductivity, and diffusion coefficients. The collision cross sections required for these properties have been recomputed herein using the same molecular data used previously by Yos (refs. 7,8, and 9). The computational techniques employed in the calculations are described in references 30 and 31 which give details of the NATA (Nonequilibrium Arc Tunnel Analysis) code (ref. 32). In NATA, the average collision cross sections $\pi\overline{\Omega}_{ij}^{(l,s)}$ for the collisions between species i and j are calculated from basic cross section data as functions of temperature and gas composition for each pair of species in the mixture. The basic data are either in tabular form or are given as simple analytical functions of temperature or composition. NATA contains twelve methods or options for calculating the cross sections $\pi\overline{\Omega}_{ii}^{(1,1)}$, $\pi\overline{\Omega}_{ii}^{(2,2)}$, and B_{ij}^{*} (the ratio of cross sections). The options include using the Coulomb cross section for the electrons and ions plus exponential potential (ref. 33) and Lennard-Jones (6-12) potential (ref. 34) for neutral species in high and low temperature ranges, respectively. The formulas employed in NATA to compute the transport properties from the collision cross sections are obtained from an approximation (ref. 35) to the rigorous first-order Chapman-Cowling expressions.

Single Species Transport Properties

The viscosity μ_i and frozen† thermal conductivity $K_{f,i}$ of a gas containing a single molecular species are given, to a good approximation, by the formulas (ref. 34, Chapters VII and VIII):

$$\mu_i = \frac{5}{16}\frac{\sqrt{\pi m_i kT}}{\pi\overline{\Omega}_{ii}^{(2,2)}}, \qquad \frac{gm}{cm-sec} \tag{17a}$$

$$= 2.6693\times 10^{-5}\frac{\sqrt{M_i T}}{\pi\overline{\Omega}_{ii}^{(2,2)}}, \qquad \frac{gm}{cm-sec} \tag{17b}$$

$$K_{f,i} = K_{tr,i} + K_{int,i} \tag{18a}$$

with

$$K_{tr,i} = \frac{75}{64}\frac{k\sqrt{\pi kT/m_i}}{\pi\overline{\Omega}_{ii}^{(2,2)}}, \qquad \frac{erg}{cm-sec-K} \tag{18b}$$

$$= 1.9891\times 10^{-4}\frac{\sqrt{T/M_i}}{\pi\overline{\Omega}_{ii}^{(2,2)}}, \qquad \frac{cal}{cm-sec-K} \tag{18c}$$

$$= \frac{15}{4}\frac{\mu_i R_{univ}}{M_i}, \qquad \frac{cal}{cm-sec-K} \tag{18d}$$

† See Appendix A for various definitions

and

$$K_{int,i} = \frac{3}{8}\left[\frac{C_{p,i}}{R_{univ}} - \frac{5}{2}\right]\frac{k\sqrt{\pi kT/m_i}}{\pi\overline{\Omega}_{ii}^{(1,1)}}, \qquad \frac{erg}{cm-sec-K} \tag{18e}$$

$$= 6.3605\times10^{-5}\,\frac{\pi\sqrt{T/M_i}}{\pi\overline{\Omega}_{ii}^{(1,1)}}\left[\frac{C_{p,i}}{R_{univ}} - \frac{5}{2}\right], \qquad \frac{cal}{cm-sec-K} \tag{18f}$$

$$= R_{univ}\frac{\mu_i}{M_i}\left[\frac{\rho D_{ii}}{\mu_i}\right]\left[\frac{C_{p,i}}{R_{univ}} - \frac{5}{2}\right], \qquad \frac{cal}{cm-sec-K} \tag{18g}$$

where $K_{tr,i}$ is the translational component of the thermal conductivity and $K_{int,i}$ is the component of thermal conductivity resulting from the diffusion of internal excitation energy of the molecules. In equations (17a) through (18g), m_i is the molecular mass in gm, k is Boltzmann's constant ($1.38\times10^{-16}\ erg/K$), T is the gas temperature in K, $\pi\overline{\Omega}_{ii}^{(l,l)}$ are average collision cross-sections for the molecules in Å^2, (where $1\ \text{Å} = 10^{-8}\ cm$), M_i is the molecular weight in $gm/gm-mole$, $R_{univ} = 1.987\ cal/gm-mole-K$, $C_{p,i}$ is the specific heat at constant pressure in $cal/gm-mole-K$, ρ is the density in gm/cm^3, and D_{ii} is the coefficient of self diffusion in cm^2/sec.

From equations (18a), (18d), and (18g), the frozen thermal conductivity may also be expressed as

$$K_{f,i} = \frac{R_{univ}\mu_i}{M_i}\left[\frac{15}{4} + \left[\frac{\rho D_{ii}}{\mu_i}\right]\left[\frac{C_{p,i}}{R_{univ}} - \frac{5}{2}\right]\right] \tag{19}$$

The factor $(\rho D_{ii}/\mu_i)$ appearing in equations (18g) and (19) is the reciprocal Schmidt number and is related to the collision cross sections $\pi\overline{\Omega}_{ii}^{(l,l)}$ through the relation (ref. 34)

$$\frac{\rho D_{ii}}{\mu_i} = \frac{6}{5}\frac{\pi\overline{\Omega}_{ii}^{(2,2)}}{\pi\overline{\Omega}_{ii}^{(1,1)}} \tag{20}$$

with D_{ii} defined as

$$D_{ii} = \frac{3}{8}\frac{\sqrt{\pi m_i kT}}{\pi\overline{\Omega}_{ii}^{(1,1)}}\left[\frac{1}{\rho}\right], \qquad \frac{cm^2}{\text{sec}} \tag{21a}$$

$$= 2.6280\times10^{-3}\,\frac{\pi\sqrt{T^3/M_i}}{\pi\overline{\Omega}_{ii}^{(1,1)}p}, \qquad \frac{cm^2}{\text{sec}} \tag{21b}$$

where p is the pressure in atm. The coefficient of self-diffusion D_{ii}, must be regarded as somewhat artificial. It is more correct to regard it as a limiting form of the coefficient of binary diffusion. The ratio $\pi\overline{\Omega}_{ii}^{(2,2)}/\pi\overline{\Omega}_{ii}^{(1,1)}$ appearing in equation (20) is a very slowly varying function of temperature, T, and hence $\rho D_{ii}/\mu_i$ is very nearly constant. This factor appearing in equation (19) has a value of unity in the Eucken correction (ref. 34) and is close to 1.32 for the Lennard-Jones potential over a large temperature range (ref. 36).

The collision cross sections $\pi\overline{\Omega}_{ii}^{(l,l)}$ or $\pi\overline{\Omega}_{ij}^{(l,s)}$‡ , in general, are the weighted

‡ The collision cross sections designated here as $\pi\overline{\Omega}_{ij}^{(l,s)}$ are the same as $\pi\sigma^2\Omega_{ij}^{(l,s)*}$ given in reference 34 and as $\overline{\Omega}_{ij}^{(l,s)}$ given in reference 31

averages of the cross sections for collisions between species i and j. These have been defined (refs. 7,8 and 9) as

$$\pi\overline{\Omega}_{ij}^{(l,s)} = \frac{\int_0^\infty \int_0^\pi exp(-\gamma^2)\gamma^{2s+3}(1-\cos^l\chi)4\pi\sigma_{ij}\sin\chi d\chi d\gamma}{\int_0^\infty \int_0^\pi \exp(-\gamma^2)\gamma^{2s+3}(1-\cos^l\chi)\sin\chi d\chi d\gamma} \tag{22}$$

where $\sigma_{ij} = \sigma_{ij}(\chi,g)$ is the differential scattering cross section for the pair (i,j), χ is the scattering angle in the center of mass system, g is the relative velocity of the colliding particles, and $\gamma = ([m_i m_j/2(m_i+m_j)kT]^{1/2})g$ is the reduced velocity. For collisions between the similar species, equation (22) yields $\pi\overline{\Omega}_{ii}^{(l,l)}$ required in equations (17) and (18).

The collision cross sections $\pi\overline{\Omega}_{ii}^{(1,1)}$ and $\pi\overline{\Omega}_{ii}^{(2,2)}$ employed here are the same as those used by Yos (refs. 7,8,9). The cross sections for the neutral species N, N_2, NO, O, and O_2 were taken from the tabulations of Yun et al. (ref. 37), for temperatures up to 15,000 K. Above 15,000 K, the cross sections for atomic N were obtained by extending Yun's calculations to 30,000 K using the same input data and techniques as were used in his work. The cross sections for the remaining species N_2, NO, O and O_2 were extrapolated to roughly 30,000 K assuming the same temperature dependence as calculated for N.

For the ionized species, the calculations used effective Coulomb cross sections chosen to make the computed transport properties for a fully ionized gas agree with the correct theoretical results (ref. 38) as discussed in references 7 and 9. The specific formulas used in the calculations are

$$\pi\overline{\Omega}_{ee}^{(2,2)} = 1.29Q_c \quad \text{for } \textit{electrons} \tag{23a}$$

$$\pi\overline{\Omega}_{ii}^{(2,2)} = 1.36Z^4Q_c \quad \text{for } \textit{ions} \tag{23b}$$

$$\pi\overline{\Omega}_{ee}^{(1,1)} = \pi\overline{\Omega}_{ii}^{(1,1)} = 0.795Z^4Q_c \quad \text{for } \textit{electrons} \text{ and } \textit{ions} \tag{23c}$$

where $Z = 1$ for singly ionized species and

$$Q_c = \frac{e^4}{(kT)^2}\ln\Lambda \tag{23d}$$

The shielding parameter Λ is defined as

$$\Lambda = \left[\frac{9(kT)^3}{4\pi e^6 n_e} + \frac{16(kT)^2}{e^4 n_e^{2/3}}\right]^{1/2} \tag{23e}$$

$$= \left[2.09\times10^{-2}\left[\frac{T^4}{10^{12}p_e}\right] + 1.52\left[\frac{T^4}{10^{12}p_e}\right]^{2/3}\right]^{1/2} \tag{23f}$$

where T is the temperature in K and $p_e = n_e kT$ is the electron pressure in atm. In equation (22d), $e = 4.8\times10^{-10}\,esu$ is the electron charge. Equation (23) is applicable for electron pressures of the order 1 atm or below and becomes less accurate as the electron pressure increases above atmospheric (ref. 38).

In the present report, the transport properties of the ionic species are provided for a nominal electron pressure of $p_e = 1$ atm. For any other electron pressure, it will be necessary to correct the tabulated transport properties of the ionic species according to the formula

$$\frac{\mu_i(p_e)}{\mu_i(1\ atm)} = \frac{K_{f,i}(p_e)}{K_{f,i}(1\ atm)} = \frac{K_{tr,i}(p_e)}{K_{tr,i}(1\ atm)} = \frac{K_{int,i}(p_e)}{K_{int,i}(1\ atm)} = \frac{\ln \Lambda(1\ atm)}{\ln \Lambda(p_e)}$$

$$= \frac{\ln\left[2.09\times 10^{-2}\left[\frac{T}{1000}\right]^4 + 1.52\left[\frac{T}{1000}\right]^{8/3}\right]}{\ln\left[2.09\times 10^{-2}\left[\frac{T}{1000p_e^{1/4}}\right]^4 + 1.52\left[\frac{T}{1000p_e^{1/4}}\right]^{8/3}\right]} \tag{24a}$$

Similarly, the collision cross sections $\pi\overline{\Omega}_{ij}^{(l,s)}$ (for the pair of species where both are ions or electrons or a combination of the two) for any other electron pressure p_e may be obtained from the values provided herein for $p_e = 1\ atm$ by employing the relation

$$\frac{\pi\overline{\Omega}_{ij}^{(l,s)}(p_e)}{\pi\overline{\Omega}_{ij}^{(l,s)}(1\ atm)} = \frac{\ln \Lambda(p_e)}{\ln \Lambda\ (1\ atm)}$$

$$= \frac{\ln\left[2.09\times 10^{-2}\left[\frac{T}{1000p_e^{1/4}}\right]^4 + 1.52\left[\frac{T}{1000p_e^{1/4}}\right]^{8/3}\right]}{\ln\left[2.09\times 10^{-2}\left[\frac{T}{1000}\right]^4 + 1.52\left[\frac{T}{1000}\right]^{8/3}\right]} \tag{24b}$$

Equation (24b) is also applicable for $i=j$ (single species).

In calculating the contribution $K_{int,i}$ of the internal energy states to the thermal conductivity for the atomic species N and O, the diffusion cross section $\pi\overline{\Omega}_{ii}^{(1,1)}$ in equations (18e) or (18f) has been set equal to the corresponding charge-exchange cross section for the atom and atomic ion (refs. 8 and 39). As discussed in reference 7, this approximation allows for the effects of excitation exchange in reducing the contribution of internal energy states to the thermal conductivity in a gas of identical atoms.

The individual species viscosities and thermal conductivities computed using equations (17) and (18) have been curve fitted herein as a function of temperature by employing the following relations

$$\mu_i = e^{E_{\mu_i}} T^{[A_{\mu_i}(\ln T)^3 + B_{\mu_i}(\ln T)^2 + C_{\mu_i}\ln T + D_{\mu_i}]}, \quad \frac{gm}{cm-sec} \tag{25}$$

$$K_{f,i} = e^{E_{K_{f,i}}} T^{[A_{K_{f,i}}(\ln T)^3 + B_{K_{f,i}}(\ln T)^2 + C_{K_{f,i}}\ln T + D_{K_{f,i}}]}, \quad \frac{cal}{cm-sec-K} \tag{26}$$

The curve-fit coefficients appearing in equations (25) and (26) are given in tables IV and V for the 11 chemical species. These coefficients yield values of the viscosity and frozen thermal conductivity of ionic species at a nominal electron pressure of 1 *atm* and should be corrected for any other electron pressure (or number density) by using equation (24a).

Figure 4 displays typical results from the viscosity curve fit (eq. (25)) of equation (17) for some of the neutral and charged species. The frozen thermal conductivity curve fit (eq. (26)) of equations (19) through (21) is shown in figure 5 for the same species. It may be noticed from these figures (and in tables IV and V) that a higher order curve is needed for the charged species because of the inflection of the viscosity

and thermal conductivity curves at low temperatures. Higher order curve fits are also needed for the thermal conductivity of the neutral molecular species.

Transport Properties of Multicomponent Mixtures

Rigorous kinetic theory formulas which have been derived directly from a solution of the Boltzmann equation using the classical Chapman-Enskog procedure (refs. 33 and 40) are available for obtaining the transport properties of a gas mixture from the molecular constituent species. In the first Chapman-Enskog approximation, formulas for both the viscosity and translational component of thermal conductivity, $K_{tr,i}$, of a gas mixtures are of the general form

$$[\mu^{(1)} \text{ or } K_{tr}^{(1)}]_{mixture} = -\frac{\begin{vmatrix} A_{11} & \cdots & A_{1v} & x_1 \\ \vdots & & \vdots & \vdots \\ A_{v1} & \cdots & A_{vv} & x_v \\ x_1 & \cdots & x_v & 0 \end{vmatrix}}{|A_{ij}|} \tag{27}$$

where x_i is the mole fraction of the ith species, $v\ (\equiv NS)$ is the total number of species present in the mixture, and the matrix elements A_{ij} can be expressed in the form

$$A_{ij} = A_{ji} = -x_i x_j a_{ij} + \delta_{ij}\left(x_i A_i + \sum_{l=1}^{v} x_i x_l a_{il}\right) \tag{28}$$

where $a_{ij}=a_{ji}$ and δ_{ij} is the Kronecker delta. Elements A_i and a_{ij} are defined subsequently. The superscript 1 on μ or K_{tr} indicates that equation (27) is the first Chapman-Enskog approximation for the transport property. Further details for obtaining the transport properties by employing the first Chapman-Enskog approximation are given in reference 35. In principle, the problem of calculating the transport coefficients for a given mixture consists of two parts: first, the determination of the collision cross sections $\pi\overline{\Omega}_{ij}$ for all possible pairs of species (i,j); and second, the evaluation of the Chapman-Enskog formulas. The amount of computation required to evaluate the mixture transport properties is greatly reduced if approximations to the complete Chapman-Enskog formulas are employed. Reference 7 has provided approximate formulas for the transport properties based on the relations developed in references 41, 42, and 43. Earlier, references 10, 11, and 44, and more recently, references 12 and 45 have also provided approximations to the Chapman-Enskog formulas. These are apparently the most satisfactory of the many simplifying approximations for the mixture viscosity and thermal conductivity which have been suggested by various authors. However, effects of the elements A_{ij} in the Chapman-Enskog formula are completely neglected in Brokaw's approximation (ref. 42) so that this approximation always gives too large a value for the transport properties. In the Buddenberg-Wilke (refs. 10 and 44) and Mason-Saxena (ref. 11) formulas, the effects of these elements are accounted for by means of a single empirical constant which is assumed to be the

same for all gas mixtures. The approximation used by Peng and Pindroh (ref. 41) represents an attempt to take account of the nondiagonal elements explicitly to first order at the expense of a somewhat increased calculational effort. Armaly and Sutton (refs. 12 and 45) neglected the nondiagonal matrix elements A_{ij} in a manner similar to Brokaw (ref. 42). However, they did not force the value of A_{ij}^*, defined as

$$A_{ij}^* = \frac{\overline{\Omega}_{ij}^{(2,2)}}{\overline{\Omega}_{ij}^{(1,1)}} \tag{29}$$

to be equal to 5/3 and 5/2 in their approximations for viscosity and thermal conductivity, respectively.† They assigned different values to A_{ij}^* for ion-atom and neutral atom-molecule interactions. From the computer time, storage, and simplicity point of view, references 10 and 11 would appear to be adequate for non-ionized gas mixtures, whereas references 12 and 45 would be useful for computing the viscosity and translational component of thermal conductivity for an ionized gas mixture.

In all the approximations to the Chapman-Enskog formulas for viscosity and translational thermal conductivity discussed thus far, the transfer of momentum or energy from one species to another by collisions has been either neglected or has been accounted for by an empirical constant. This transfer process, which is represented by the nondiagonal elements A_{ij} in the Chapman-Enskog formula (eq. (27)), has the effect of making the less conductive species in the mixture carry a larger fraction of the transport. This process, therefore, reduces the overall conductivity of the mixture below the value which it would have if the transfer process were neglected.

In reference 35, Yos obtained approximations to the Chapman-Enskog formulas which account for the effects of the above mentioned transfer process between different species. These cross sections reproduce the results of the first Chapman-Enskog formula (eqs. (27) and (28)) to within a fraction of a percent for all cases considered in reference 35 and are also simpler to use than the latter. Based on the cross sections developed by Yos (ref. 35), the following formulas may be used to compute viscosity and the translational component of thermal conductivity

$$[\mu^{(1)} \text{ or } K_{tr}^{(1)}] = \frac{\sum_{i=1}^{NS} x_i/(A_i + a_{av})}{1 - a_{av}\sum_{i=1}^{NS} x_i/(A_i + a_{av})} \tag{30}$$

Here, NS is the number of species in the gas, x_i is the mole fraction of the ith species, and a_{av} is an average value of the nondiagonal matrix elements a_{ij} contained in equation (28) which is defined as

$$a_{av} = \frac{\sum_{i,j=1}^{NS} x_i x_j \left[\frac{1}{A_i} - \frac{1}{A_j}\right]^2 a_{ij}}{\sum_{i,j=1}^{NS} x_i x_j \left[\frac{1}{A_i} - \frac{1}{A_j}\right]^2} \tag{31a}$$

with

† With $A^* = 5/3$ and $5/2$, A_{ij} becomes identically equal to zero in the Chapman-Enskog formula.

$$A_i = \sum_{l=1}^{NS} x_l A_{il} \tag{31b}$$

For the viscosity, the quantities a_{ij} and A_{ij} appearing in equations (31a) and (31b) are defined as

$$a_{ij} = \frac{N_A}{(M_i + M_j)}[2\Delta_{ij}^{(1)} - \Delta_{ij}^{(2)}] \tag{32a}$$

$$A_{il} = \frac{N_A}{M_i}\Delta_{il}^{(2)} \tag{32b}$$

For translational thermal conductivity, the above quantities are defined as

$$a_{ij} = \left[\frac{2}{15k}\right]\frac{M_i M_j}{(M_i + M_j)^2}\left[\left[\frac{33}{2} - \frac{18}{5}B_{ij}^*\right]\Delta_{ij}^{(1)} - 4\Delta_{ij}^{(2)}\right] \tag{33a}$$

and

$$A_{il} = \frac{2}{15k(M_i + M_l)^2}\left\{8M_i M_l \Delta_{il}^{(2)} + (M_i - M_l)\left[9M_i - \frac{15}{2}M_l + \frac{18}{5}B_{il}^* M_l\right]\Delta_{il}^{(1)}\right\} \tag{33b}$$

In these equations, M_i is the molecular weight of the ith species, $N_A = 6.0225\times 10^{23}$ *molecules/gm−mole* is Avogadro's number, and $k = 1.3805\times 10^{-16}$ *erg/K* is Boltzman's constant. The remaining quantities are defined as

$$\Delta_{ij}^{(1)} = \frac{8}{3}\left[\frac{2M_i M_j}{\pi N_A kT(M_i + M_j)}\right]^{1/2}\pi\overline{\Omega}_{ij}^{(1,1)} \tag{34}$$

$$\Delta_{ij}^{(2)} = \frac{16}{5}\left[\frac{2M_i M_j}{\pi N_A kT(M_i + M_j)}\right]^{1/2}\pi\overline{\Omega}_{ij}^{(2,2)} \tag{35}$$

$$B_{ij}^* = \frac{5\overline{\Omega}_{ij}^{(1,2)} - 4\overline{\Omega}_{ij}^{(1,3)}}{\overline{\Omega}_{ij}^{(1,1)}} \tag{36}$$

and the collision integrals $\pi\overline{\Omega}_{ij}^{(l,s)}$ are weighted averages of the cross sections defined through equation (22).

The frozen thermal conductivity K_f employed in defining the frozen Prandtl and Lewis numbers† can be obtained from the modified Eucken approximation (ref. 43)

$$K_f = K_{tr} + K_{int} \tag{37}$$

where K_{tr} is the translational component of the thermal conductivity given by equations (30) to (36) and K_{int} is the component of thermal conductivity resulting from the internal excitation energy of the molecules, defined (ref. 7) as

$$K_{int} = k\sum_{i=1}^{NS}\left[\frac{\left[\frac{M_i C_{p,i}}{kN_A} - \frac{5}{2}\right]x_i}{\left[\sum_{j=1}^{NS} x_j \Delta_{ij}^{(1)}\right]}\right] \tag{38}$$

† See Appendix A for various definitions

Here, $C_{p,i}$ is the specific heat at constant pressure of the ith species.

The binary diffusion coefficient D_{ij} needed to obtain the binary and multicomponent Lewis numbers (refs. 13, 14, and 34) is obtained from the complete first Chapman-Enskog approximation (ref. 34):

$$D_{ij} = \frac{\bar{D}_{ij}}{p} = \frac{kT}{p\Delta_{ij}^{(1)}} \quad , \qquad cm^2/sec \tag{39a}$$

with

$$\bar{D}_{ij} = \frac{kT}{\Delta_{ij}^{(1)}} \quad , \qquad cm^2\text{-}atm/sec \tag{39b}$$

Here p is the pressure in atmospheres. Equation (39b) for $\bar{D}_{ij}$ has been curve fitted in the present work by using the expression

$$\bar{D}_{ij} = e^{D_{\bar{D}_{ij}} T^{[A_{\bar{D}_{ij}}(\ln T)^2 + B_{\bar{D}_{ij}} \ln T + C_{\bar{D}_{ij}}]}} \quad , \qquad cm^2\text{-}atm/sec \tag{40a}$$

where T is the temperature in K. The curve-fit coefficients of equation (40a) are given in table VI for the different interactions occurring in the 11-species air model.

The values of $\bar{D}_{ij}$ obtained from equation (40a) with the curve-fit coefficients given in table VI are for a nominal electron pressure of 1 atm. If the pair of interacting species are both ions, both electrons, or any combination of the two, then $\bar{D}_{ij}$ may be corrected for any other electron pressure by employing:

$$\bar{D}_{ij}(P_e) = \bar{D}_{ij}(1\,atm) \frac{\ln \left[2.09\times 10^{-2} \left[\frac{T}{1000} \right]^4 + 1.52 \left[\frac{T}{1000} \right]^{8/3} \right]}{\ln \left[2.09\times 10^{-2} \left[\frac{T}{1000 p_e} \right]^4 + 1.52 \left[\frac{T}{1000 p_e} \right]^{8/3} \right]} \tag{40b}$$

If the approximations of references 41 through 43 are employed in place of the more exact formulas given by equations (30) through (36)† , then the following approximate formulas for the mixture viscosity and thermal conductivity may be used (ref. 7):

$$\mu_{mixture}^{(1)} = \sum_{i=1}^{NS} \left[\frac{\frac{M_i}{N_A} x_i}{\sum_{j=1}^{NS} x_j \Delta_{ij}^{(2)}} \right] \tag{41}$$

$$[K_{ir}^{(1)}]_{mixture} = \frac{15}{4} k \sum_{i=1}^{NS} \left[\frac{x_i}{\sum_{j=1}^{NS} \alpha_{ij} x_j \Delta_{ij}^{(2)}} \right] \tag{42a}$$

where $\Delta_{ij}^{(2)}$ is given by equation (35) and α_{ij} is defined as

$$\alpha_{ij} = 1 + \frac{[1-(M_i/M_j)][0.45-2.54(M_i/M_j)]}{[1+(M_i/M_j)]^2} \tag{42b}$$

† The approximations of references 41 through 43 may be valid only for the range of conditions for which they have been developed and not for general application because of the very approximate analysis of the nondiagonal matrix elements A_{ij} of equation (27).

To obtain the viscosity μ and the translational component of thermal conductivity K_{tr} of a gas mixture from either the more exact equations (30) through (36) or from the approximate relations in equations (41) through (42), the binary collision cross sections $\pi\overline{\Omega}_{ij}^{(l,s)}$ and their ratios are needed in equations (34) through (36). These cross sections, defined by equation (22), are the same as those used by Yos (refs. 7,8, and 9). In addition to the formulas given by equation (23) for the Coulomb collision integrals, the following relations are also employed:

$$\pi\overline{\Omega}_{el}^{(1,1)} = 0.795Z^4Q_c \tag{43a}$$

$$\pi\overline{\Omega}_{el}^{(2,2)} = 1.29Q_c \tag{43b}$$

where the subscripts e and I represent electrons and ions, respectively, and Z and Q_c are defined in equation (23d).

The NATA code (refs. 30,31, and 32) employed to obtain the collision cross sections, $\pi\overline{\Omega}_{ij}^{(l,s)}$, contains default provisions for estimating some cross sections if they are not specified explicitly in the built-in database or the input. The defaults are summarized as

(i) If both species are ions, then the Coulomb cross sections given by equations (23) and (43) are used.

(ii) If one species is neutral and the other ionized, then the formula

$$\pi\overline{\Omega}_{ij}^{(l,s)} = A^{(l,s)}T^{-0.4} \tag{44a}$$

is employed with the constants $A^{(l,s)}$ defined in the code.

(iii) If both species are neutral and are unlike, then the cross sections are estimated using the simple mixing rule

$$\pi\overline{\Omega}_{ij}^{(l,s)} = \frac{1}{4}\left(\sqrt{\pi\overline{\Omega}_{ij}^{(l,s)}} + \sqrt{\pi\overline{\Omega}_{ij}^{(l,s)}}\right)^2 \tag{44b}$$

The built-in data in NATA specify steps for calculating the cross sections for the like-like interactions of ten species ($e^-, N_2, O_2, N, O, NO, NO^+, N^+, O^+$, and N_2^+) and for those unlike interactions for which experimental or theoretical cross sections are available in the literature. The cross sections for O_2^+ are taken to be the same as those for N_2^+ in these calculations. NATA contains twelve methods or options for calculating $\pi\overline{\Omega}_{ij}^{(1,1)}$, $\pi\overline{\Omega}_{ij}^{(2,2)}$, and B_{ij}^* which are described in detail in references 30 through 32. Note that the accuracy of the calculated transport properties is largely determined by the accuracy of the input data for the cross-section integrals. A brief discussion of the values employed in the present study is given in reference 7. Reference 46 provides a comparison between theory and experiment for the thermal conductivity of nitrogen up to temperatures of 14000 K. Fairly good agreement between the two is shown there.

Figures 6 and 7 give viscosity and frozen thermal conductivity values, respectively, obtained for equilibrium air at 1 *atm* by employing the presently computed collision cross sections for the constituent species. The present calculations employ equation (41) for the calculation of mixture viscosity and equations (37), (38), and (42) for the mixture frozen thermal conductivity. In addition, the collision cross sections used are nearly identical to those obtained in reference 9. The mixing laws employed for the viscosity and thermal conductivity shown in figures 6 and 7 are accurate for sub-ionization temperatures (less than 9000 K at 1 atm) only. For ionized flows, more accurate mixing laws of the type given by equation (30) should be employed. Figures

6 and 7 also include viscosity and thermal conductivity values from other researchers for comparison. In these figures, the predictions of Peng and Pindroh (ref. 41) and Esch et al. (ref. 47) are based on the Buddenberg-Wilke (ref. 44) type of mixture law and have the same level of approximation as the present calculations. The mixture laws employed by Hansen (ref. 29) contain a somewhat lower level of approximation. In Hansen's work, the viscosity is computed by using the simple summation formula for a mixture of hard sphere molecules, whereas a linearized expression with Eucken's assumption (ref. 34) is employed for the frozen thermal conductivity. The viscosity values obtained in the present work are in good agreement (fig. 6) with the values obtained by Peng and Pindroh (ref. 41) and Esch et al. (ref. 47), presumably due to the similar mixing laws employed. Hansen's (ref. 29) predictions are lower, especially at higher temperatures. Even with the beginning of dissociation of molecular nitrogen at about 4000 K (when the dissociation of molecular oxygen is almost complete), Hansen's values of viscosity are not much different from the Sutherland's law. For the frozen thermal conductivity (fig. 7), the present values are in agreement with those obtained by Peng and Pindroh (ref. 41) up to temperatures of about 9000 K. The values obtained by Esch et al. (ref. 47) deviate from the present values beyond 6000 K. This may be due to the constant cross-sectional values employed for the ionized species in the 8000 to 15000 K temperature range in reference 47. Hansen's predictions of thermal conductivity are lower than the other data and are closer to the Sutherland values up to temperatures of about 4000 K. Again, the differences between the present computations and those of Hansen are presumably due to the somewhat more rigorous mixing laws employed herein.

There are 121 possible binary interactions for the dissociating air having eleven species. Therefore, 121 values of each of the collision cross sections $\pi\overline{\Omega}_{ij}^{(1,1)}$, $\pi\overline{\Omega}_{ij}^{(2,2)}$ and the collision cross-section ratio B_{ij}^{*} are required to evaluate the transport properties. By use of the symmetrical equality, i.e. $(i,j) = (j,i)$, only 66 values of each cross section and cross-section ratio are required. These values have been curve fit in the present study as a function of temperature for a nominal electron pressure of 1 *atm* using the following relations

$$\pi\overline{\Omega}_{ij}^{(1,1)} = e^{D_{\overline{\Omega}_{ij}^{(1,1)}} T^{\left[A_{\overline{\Omega}_{ij}^{(1,1)}}(\ln T)^2 + B_{\overline{\Omega}_{ij}^{(1,1)}}\ln T + C_{\overline{\Omega}_{ij}^{(1,1)}}\right]}}, \quad \text{Å}^2 \tag{45}$$

$$\pi\overline{\Omega}_{ij}^{(2,2)} = e^{D_{\overline{\Omega}_{ij}^{(2,2)}} T^{\left[A_{\overline{\Omega}_{ij}^{(2,2)}}(\ln T)^2 + B_{\overline{\Omega}_{ij}^{(2,2)}}\ln T + C_{\overline{\Omega}_{ij}^{(2,2)}}\right]}}, \quad \text{Å}^2 \tag{46}$$

$$B_{ij}^{*} = e^{D_{B_{ij}^{*}} T^{\left[A_{B_{ij}^{*}}(\ln T)^2 + B_{B_{ij}^{*}} + C_{B_{ij}^{*}}\right]}} \tag{47}$$

For electron pressures different from unity, the formula given by equation (24b) is used to correct the cross sections for the ionic species. No such correction is required for the cross-section-ratio parameter B_{ij}^{*}.

Curve-fit coefficients appearing in equations (45) through (47) are given in Table VII through IX for the various interactions in an 11-species air model. Figure 8 illustrates some typical curve fits obtained by employing equation (40a) and equations (45) through (47) with the associated constants. The figure compares the computed values of binary diffusion coefficient, collision integrals, and collision integral ratio with the resulting curve fit for different interaction pairs of neutral and ionized species, including electrons. The collision integral ratio, B_{ij}^{*}, is almost constant with temperature as shown in the figure and was fitted with the lower order curve fit where possible. However, the collision integrals $\pi\overline{\Omega}_{ij}^{(l,s)}$ for the charged species pairs exhibit more complex

behavior and require higher order curve fits.

The transport properties of a multi-temperature gas mixture may be obtained by following the approaches of references 20 and 48. These references have used equations (41) and (42) for the calculation of mixture viscosity and translational thermal conductivity. The collision integrals for heavy particles in these equations are evaluated by using the heavy particle translational temperature, whereas those for electrons with any other partner are obtained by using the electron temperature. With these modifications, equations (41) and (42) can be written for an 11-species gas mixture as

$$\mu_{mixture} = \sum_{i=1}^{10} \left[\frac{\frac{M_i}{N_A} x_i}{\sum_{j=1}^{10} x_j \Delta_{ij}^{(2)}(T) + x_e \Delta_{ie}^{(2)}(T_e)} \right] + \frac{\frac{M_e}{N_A} x_e}{\sum_{j=1}^{11} x_j \Delta_{ej}^{(2)}(T_e)} \tag{48}$$

$$(K_{tr}^*)_{mixture} = \frac{15}{4} k \sum_{i=1}^{10} \left[\frac{x_i}{\sum_{j=1}^{10} \alpha_{ij} x_j \Delta_{ij}^{(2)}(T) + 3.54 x_e \Delta_{ie}^{(2)}(T_e)} \right] \tag{49}$$

where α_{ij} is still obtained from equation (42b). Note that the above definition of K_{tr}^* does not include contributions due to electron-heavy particle and electron-electron collisions. These contributions, defined by K_e, are given later. The approach outlined here may also be used to obtain the mixture viscosity and thermal conductivity from the more exact expressions in equations (30) through (36). Equation (38) for the internal thermal conductivity needs to be modified for the multi-temperature formulation. The contributions resulting from the excitation of different internal energy modes can not be lumped together into a single term K_{int} for such a formulation. Further, equation (37) no longer can be used to obtain a frozen thermal conductivity for the mixture. The relation given in equation (37) may be used to obtain a frozen thermal conductivity with only the rotational mode contributing to the internal energy at the translational temperature. In general, there are four components of the internal thermal conductivity, similar to the molecular specific heat (fig. 2). Using these components, the k th component of the overall heat flux vector can be expressed as

$$q^k = -(K_{tr}^* + K_{rot}) \frac{\partial T}{\partial x^k} - K_{vib} \frac{\partial T_v}{\partial x^k} - K_{el} \frac{\partial T_{el}}{\partial x^k} - K_e \frac{\partial T_e}{\partial x^k} + \sum_{i=1}^{NS} \rho_i h_i V_i^k \tag{50a}$$

where K_{tr}^* is the translational thermal conductivity defined previously by equation (49) and K_{rot}, K_{vib} and K_{el} are the rotational, vibrational, and electronic thermal conductivities, respectively, associated with these internal energy modes (ref. 49). Also, K_e is the thermal conductivity of electrons, T is the translational-rotational temperature, T_v is the vibrational temperature, T_{el} is the electronic excitation temperature, T_e is the electron temperature, x^k is the k th component in a general orthogonal coordinate system, and the last term is the diffusive component of the heat flux vector. Further details of the heat flux vector q^k and other definitions are given in appendix A. Two other heat flux vectors are required in describing the conservation equations for the electron energy and the vibrational energy (ref. 48). The electron heat-flux vector q_e^k and the vibrational heat-flux vector q_v^k are defined in appendix C. The thermal conductivities required to evaluate these flux vectors are obtained from the electron-electron and molecule-molecule collisions. These thermal conductivities are also

defined in appendix C. In the diffusive heat flux component, ρ_i, h_i, and V_i^k are the density, enthalpy and diffusion velocity of species i, respectively. For a two-temperature model, equation (50a) may be written (refs. 19 and 20) as

$$q^k = -(K_{tr}^* + K_{rot})\frac{\partial T}{\partial x^k} - (K_{vib} + K_{el} + K_e)\frac{\partial T_{ve}}{\partial x^k} + \sum_{i=1}^{NS} \rho_i h_i V_i^k \tag{50b}$$

Different components of the internal thermal conductivity appearing in equation (50) can be evaluated from equation (38) by appropriate modifications for these components. For example, K_{rot} can be obtained from

$$(K_{rot})_{\substack{Partial \\ Excitation}} = k\sum_{i=1}^{NS}\left[\frac{\left[\frac{M_i}{N_A}\frac{C_{p,i}(T_{rot})}{k} - \frac{5}{2}\right]x_i}{\sum_{j=1}^{NS} x_j \Delta_{ij}^{(1)}(T_{rot})}\right] \tag{51a}$$

for partial excitation of the rotational internal energy mode if the temperature is less than that needed to excite the vibrational energy mode (fig. 2). Values of specific heat at constant pressure, $C_{p,i}$, appearing in equation (51a) can be obtained from the curve-fit relation of equation (13) by employing the rotational temperature, T_{rot}, if different from the translational temperature T. When the vibrational mode begins to excite, the rotational mode is fully excited and equation (51a) becomes

$$(K_{rot})_{\substack{Full \\ Excitation}} = k\sum_{i=1}^{NS}\left[\frac{x_i}{\sum_{j=1}^{NS} x_j \Delta_{ij}^{(1)}(T_{rot})}\right] \tag{51b}$$

Similarly, expressions for K_{vib} with partial and full excitations of the vibrational energy mode may be written as

$$(K_{vib})_{\substack{Partial \\ Excitation}} = k\sum_{i=1}^{NS}\left[\frac{\left[\frac{M_i}{N_A}\frac{C_{p,i}(T_{vib})}{k} - \frac{7}{2}\right]x_i}{\sum_{j=1}^{NS} x_j \Delta_{ij}^{(1)}(T_{vib})}\right] \tag{52a}$$

and

$$(K_{vib})_{\substack{Full \\ Excitation}} = k\sum_{i=1}^{NS}\left[\frac{x_i}{\sum_{j=1}^{NS} x_j \Delta_{ij}^{(1)}(T_{vib})}\right] \tag{52b}$$

Once again, the value of $C_{p,i}$ appearing in equation (52a) can be obtained from the curve-fit relation of equation (13) by employing T_{vib}. Also, the vibrational energy mode is fully excited when the electronic contribution becomes significant (as shown in fig. 2 for the specific heat at constant pressure).

The rotational and vibrational energy modes are almost fully excited at their respective characteristic temperatures. Therefore, for rotational and vibrational temperatures greater than these characteristic temperatures, equations (51b) and (52b) can be employed to obtain K_{rot} and K_{vib}, respectively.

Expressions for K_{el} with the excitation of electronic energy mode can be written as

$$K_{el} = k \sum_{i=1}^{NS} \left[\frac{\left[\frac{M_i}{N_A} \frac{C_{p,i}(T_{el})}{k} - \frac{9}{2} \right] x_i}{\sum_{j=1}^{NS} x_j \Delta_{ij}^{(1)}(T_{el})} \right] \tag{53}$$

In equation (53), higher electronic degeneracy levels begin to contribute to K_{el} (and $C_{p,i}$, etc.) as the characteristic temperatures for the electronic excitation of those degeneracy levels are reached.

Finally, the thermal conductivity for free electrons, K_e, appearing in equation (50) may be obtained from the modified form of equation (42)

$$K_e = \frac{15}{4} \frac{k\, x_e}{\sum_{j=1}^{NS} 1.45 x_j \Delta_{ej}^{(2)}(T_e)} \tag{54}$$

This thermal conductivity results from the collisions between electrons and other species, including other electrons.

Concluding Remarks

The present work provides the reaction rate coefficients and thermodynamic and transport properties for an 11-species air model which are needed in analyzing the high energy flow environment of currently proposed and future hypersonic vehicles. Approximate and more exact formulas have been provided for computing the properties of partially ionized gas mixtures in chemical and thermal nonequilibrium around such vehicles.

The work presented here uses the best estimates of available data needed to compute properties of the 11-species air model. However, there is need for improved data, especially for air in thermochemical nonequilibrium. There is also some degree of uncertainty about reaction rate coefficients at high temperatures. Both the theoretical and experimental bases of the multi-temperature kinetic models need to be strengthened. The virial coefficient approach as compared to the partition function analysis for obtaining the thermodynamic properties at higher temperatures appears sufficient but needs further verification. For transport properties, the input data for obtaining the collision cross sections at high temperatures are not adequate.

BIBLIOGRAPHY

1. Howe, J. T., "Introductory Aerothermodynamics of Advanced Space Transportation Systems," AIAA Paper 83-0406, January 1983.
2. Walberg, G. D., "A Survey of Aeroassited Orbit Transfer," *Journal of Spacecraft and Rockets*, vol. 22, no. 1, pp. 3-18, January-February 1985.
3. Williams, R. M., "National Aerospace Plane: Technology for America's Future," *Aerospace America*, vol. 24, no. 11, pp. 18-22, November 1986.
4. Martin, J. A., "Special Section - Orbit-On-Demand Vehicle," *Aerospace America*, vol. 2, no. 2, pp. 46-58, February 1985.
5. Hansen, C. F. and S. P. Heims, "A Review of the Thermodynamic, Transport, and Chemical Reaction Rate Properties of High-Temperature Air," NACA TN 4359, July 1958.
6. Bird, G. A., in *Molecular Gas Dynamics*, p. 11, Clarendon Press, Oxford, 1976.
7. Yos, J. M., "Transport Properties of Nitrogen, Hydrogen, Oxygen, and Air to 30000 K," RAD-TM-63-7, AVCO Corp., Wilmington, Mass., March 1963.
8. Yos, J. M., "Theoretical and Experimental Studies of High-Temperature Gas Transport Properties," RAD-TR-65-7, p. Section III, Avco Corp., Wilmington, Mass., May 1965.
9. Yos, J. M., "Revised Transport Properties for High Temperature Air and Its Components," Tech. Release, Space Systems Division, AVCO Corp., Wilmington, Mass., November 1967.
10. Wilke, C. R., "A Viscosity Equation for Gas Mixtures," *Journal of Chemical Physics*, vol. 18, no. 4, pp. 517-519, 1950.
11. Mason, E. A. and S. C. Saxena, "Approximate Formula for the Thermal Conductivity of Gas Mixtures," *Physics of Fluids*, vol. 1, no. 5, p. 361, 1958.
12. Armaly, B. F. and K. Sutton, "Viscosity of Multicomponent Partially Ionized Gas Mixtures Associated with Jovian Entry," AIAA Paper 80-1495, July 1980.
13. Blottner, F. G., "Viscous Shock Layer at the Stagnation Point with Nonequilibrium Air Chemistry," *AIAA Journal*, vol. 7, no. 12, pp. 2281-2288, 1969.
14. Moss, J. N., "Reacting Viscous-Shock-Layer Solutions with Multicomponent Diffusion and Mass Injection," NASA TR R-411, June 1974.
15. Gupta, R. N. and A. L. Simmonds, "Hypersonic Low Density Solutions of the Navier-Stokes Equations with Chemical Nonequilibrium and Multicomponent Surface Slip," AIAA Paper 86-1349, June 1986.
16. Bortner, M. H., "Suggested Standard Chemical Kinetics for Flow Field Calculations - A Consensus Opinion," in *AMRAC Proceedings*, vol. 14, Part 1, pp. 569-581, Inst. Sci. Technol., Univ. of Michigan, April 1966.
17. Dunn, M. G. and S. W. Kang, "Theoretical and Experimental Studies of Reentry Plasmas," NASA CR-2232, April 1973.
18. Gupta, R. N., "Navier-Stokes and Viscous Shock-Layer Solutions for Radiating Hypersonic Flows," AIAA Paper 87-1576, June 1987.
19. Park, C., "Assessment of Two-Temperature Kinetic Model for Ionizing Air," AIAA Paper 87-1574, June 1987.

20. Gnoffo, P. A., R. N. Gupta, and J. L. Shinn, "Conservation Equations and Physical Models for Hypersonic Air Flows in Thermal and Chemical Nonequilibrium," NASA TP-2867, 1988.

21. Treanor, C. E. and P. V. Marrone, "Effects of Dissociation of the Rate of Vibrational Relaxation," *Physics of Fluids*, vol. 5, no. 9, pp. 1022-1026, 1962.

22. Marrone, P. V. and C. E. Treanor, "Chemical Relaxation with Preferential Dissociation from Excited Vibrational Levels," *Physics of Fluids*, vol. 6, no. 9, pp. 1215-1221, 1963.

23. Jaffe, R. L., "Rate Constants for Chemical Reactions in High-Temperature Non-equilibrium Air," in *Thermophysical Aspects of Re-Entry Flows*, ed. J. N. Moss and C. D. Scott, pp. 123-151, AIAA, New York, 1986.

24. Moss, J. N., V. Cuda, and A. L. Simmonds, "Nonequilibrium Effects for Hypersonic Transitional Flows," AIAA Paper 87-0404, June 1987.

25. Sharma, S. P., W. M. Huo, and C. Park, "The Rate Parameters for Coupled Vibration-Dissociation in a Generalized SSH Approximation," AIAA Paper 88-2714, June 1988.

26. McBride, B. J., S. Heimel, J. G. Ehlers, and S. Gordon, "Thermodynamic Properties to 6000 K for 210 Substances Involving the First Eighteen Elements," NASA SP-3001, 1963.

27. Browne, W. G., "Thermodynamic Properties of Some Atoms and Atomic Ions," General Electric Co., Valley Forge, Pa., Missile and Space Vehicle Dept., Eng. Phy. Tech. Memo., No. 2, 1962.

28. Browne, W. G., "Thermodynamic Properties of Some Diatoms and Diatomic Ions," General Electric Co., Valley Forge, Pa., Missile and Space Vehicle Dept., Eng. Phy. Tech. Memo., No. 8, 1962.

29. Hansen, C. F., "Approximations for the Thermodynamic and Transport Properties of High-Temperature Air," NASA TR R-50, 1959.

30. Yos, J. M., "Transport Property Calculations in the NATA Code," AVCO Tech. Release NDR-1, D210-71-JMY-13, AVCO Systems Division, August 1971.

31. Bade, W. L. and J. M. Yos, "The NATA Code - Theory and Analysis," NASA CR-2547, June 1975.

32. Yos, J. M., "Transport Property Calculations in the NATA Code, II Programming Considerations," AVCO Tech. Release NDR-1, D210-71-JMY, AVCO Systems Division, October 1971.

33. Monchick, L., "Collision Integrals for the Exponential Repulsive Potential," *Physics of Fluids*, vol. 2, no. 6, pp. 695-700, Nov.-Dec. 1959.

34. Hirschfelder, J. O., C. F. Curtiss, and R. B. Bird, in *Molecular Theory of Gases and Liquids*, John-Wiley and Sons, Inc., 1967.

35. Yos, J. M., "Approximate Equations for the Viscosity and Translational Thermal Conductivity of Gas Mixtures," Rept. AVSSD-0112-67-RM, AVCO Missile Systems Division, April 1967.

36. Svehla, R. A., "Estimated Viscosities and Thermal Conductivities of Gases at High Temperatures," NASA TR R-132, 1962.

37. Yun, K. S., S. Weissman, and E. A. Mason, "High-Temperature Transport Properties of Dissociating Nitrogen and Dissociating Oxygen," *Physics of Fluids*, vol. 5, no. 6, p. 672, June 1962.

38. Spitzer, L., in *Physics of Fully Ionized Gases*, 2nd edition, Interscience, New York, 1962.

39. Stebbings, R. F., A. C. H. Smith, and H. Ehrhardt, "Charge Transfer Between Oxygen Atoms and O^+ and H^+ Ions," *J. Geophysical Research*, vol. 69, no. 11, p. 2349, June 1964.

40. Chapman, S. and T. G. Cowling, in *The Mathematical Theory of Nonuniform Gases*, Cambridge University Press Second Edition, 1952.

41. Peng, T. C. and A. L. Pindroh, "An Improved Calculation of Gas Properties at High Temperatures: Air," Rept. No. D2-11722, Flight Tech. Dept., Aero-Space Division, Boeing Airplane Company, Seattle, Washington, February 1962.

42. Brokaw, R. S., "Approximate Formulas for the Viscosity and Thermal Conductivity of Gas Mixtures," *J. Chemical Physics*, vol. 29, no. 2, p. 391, August 1958.

43. Hirschfelder, J. O., "Heat Conductivity in Polyatomic or Electronically Excited Gases, Part II," *J. Chemical Physics*, vol. 26, no. 2, p. 282, February 1957.

44. Buddenberg, J. W. and C. R. Wilke, "Calculation of Gas Mixture Viscosities," *Ind. Eng. Chem.*, vol. 41, p. 1345, 1949.

45. Armaly, B. F. and K. Sutton, "Thermal Conductivity of Partially Ionized Gas Mixtures," AIAA Paper 81-1174, June 1981.

46. Morris, J. C., R. P. Rudis, and J. M. Yos, "Measurements of Electrical and Thermal Conductivity of Hydrogen, Nitrogen and Argon at High Temperatures," *Physics of Fluids*, vol. 13, no. 3, pp. 608-617, March 1970.

47. Esch, D. D., R. W. Pike, C. D. Engel, R. C. Farmer, and J. F. Balhoff, "Stagnation Region Heating of a Phenolic-Nylon Ablator During Return From Planetary Missions," Reacting Fluids Lab Rept., Dept. Chem. Eng., Louisiana State University, Sept. 1, 1971. (available as NASA CR-112026)

48. Lee, J. H., "Basic Governing Equations for the Flight Regimes of Aeroassisted Orbital Transfer Vehicles," in *Thermal Design of Aeroassisted Transfer Vehicles*, ed. H. F. Nelson, Progress in Astronautics and Aeronautics, Vol. 96, pp. 3-53, AIAA, New York, 1985.

49. Vincenti, W. G. and C. H. Kruger, Jr., *Introduction to Physical Gas Dynamics*, p. 86, R. E. Krieger Publishing Co., Huntington, New York, 1977.

50. Gupta, R. N., C. D. Scott, and J. N. Moss, "Slip-Boundary Equations for Multicomponent Nonequilibrium Airflow," NASA TP-2452, November 1985.

51. Blottner, F. G., "Nonequilibrium Boundary Layer Flow of Ionized Air," *AIAA J.*, vol. 2, no. 11, pp. 1921-1927, November 1964.

52. Gupta, R. N. and A. L. Simmonds, "Stagnation Flowfield Analysis for an Aeroassist Flight Experiment Vehicle," AIAA Paper 88-2613, June 1988.

Appendix A

Heat Flux, Frozen and Reactive Prandtl and Lewis Numbers, and Associated Definitions

The kth component of overall heat flux vector q^k for the dissociating and ionizing 11-species air model in a multi-temperature formulation can be expressed as†

$$q^k = -(K_{tr}^* + K_{rot})\frac{\partial T}{\partial x^k} - K_{vib}\frac{\partial T_v}{\partial x^k} - K_{el}\frac{\partial T_{el}}{\partial x^k} - K_e\frac{\partial T_e}{\partial x^k} + \sum_{i=1}^{11}\rho_i h_i V_i^k \tag{A1}$$

where the various symbols are explained in the main text after equation (50a). For thermal equilibrium conditions, equation (A1) may be written as

$$q^k = -(K_{tr}^* + K_{rot} + K_{vib} + K_{el} + K_e)\frac{\partial T}{\partial x^k} + \sum_{i=1}^{11}\rho_i h_i V_i^k \tag{A2}$$

or,

$$q^k = -K_f\frac{\partial T}{\partial x^k} + \sum_{i=1}^{11}\rho_i h_i V_i^k \tag{A3}$$

with

$$K_f = (K_{tr}^* + K_e) + K_{int} \tag{A4}$$

and

$$K_{int} = K_{rot} + K_{vib} + K_{el} \tag{A5}$$

It may also be noted that under thermal equilibrium conditions

$$K_{tr} = K_{tr}^* + K_e \tag{A6}$$

where K_{tr} is given by equation (42), K_{tr}^* is obtained from equation (49) and K_e is evaluated from equation (54). The last term in equations (A1), (A2) and (A3) represents the diffusion contribution to the heat flux vector. The diffusion mass flux of species i, J_i^k, is related to the diffusion velocity V_i^k through the relation

$$J_i^k = \rho_i V_i^k \tag{A7}$$

and for the case of binary diffusion may be expressed as (ref. 50)

$$J_i^k = -\rho D_{ij}\frac{\partial C_i}{\partial x^k} \tag{A8}$$

when the species i diffuses into any other species j. Here, C_i is the mass fraction of species i and D_{ij} is the binary diffusion coefficient. Using relation (A7) and (A8), equation (A3) can be written as

$$q^k = -K_f\frac{\partial T}{\partial x^k} - \rho\sum_{i=1}^{11}D_{ij}h_i\frac{\partial C_i}{\partial x^k} \tag{A9}$$

or,

$$q^k = -K_f\frac{\partial T}{\partial x^k} - \left[\rho\sum_{i=1}^{11}D_{ij}h_i\frac{\partial C_i}{\partial T}\right]\frac{\partial T}{\partial x^k} \tag{A10}$$

† Here we have used the sign convention that the heat flux vector is positive in the normal direction away from the surface.

or,

$$q^k = -K\frac{\partial T}{\partial x^k} \tag{A11}$$

where K is the total effective thermal conductivity defined as

$$K = K_f + \rho\sum_{i=1}^{11} D_{ij}h_i\frac{\partial C_i}{\partial T} \tag{A12}$$

or,

$$K = K_f + K_d \tag{A13}$$

with the diffusion contribution to the thermal conductivity, K_d, defined as

$$K_d = \rho\sum_{i=1}^{11} D_{ij}h_i\frac{\partial C_i}{\partial T} \tag{A14}$$

An alternate definition of the total thermal conductivity, K, is given in reference 7 as

$$K = K_f + K_r \tag{A15}$$

where K_r is the reaction thermal conductivity† defined as

$$K_r = k\sum_{l=1}^{NIR}\left[\frac{(\Delta h_l/R_{univ}T)^2}{\sum_{i=1}^{NS}[(\beta_{i,l}-\alpha_{i,l})/x_i]\sum_{j=1}^{NS}[(\beta_{i,l}-\alpha_{i,l})x_j-(\beta_{j,l}-\alpha_{j,l})x_i]\Delta_{ij}^{(1)}}\right] \tag{A16}$$

where k is the Boltzmann constant, NIR is the total number of independent reactions in the system, NS is the total number of species in the system, $\Delta h_l = \sum_{i=1}^{NS}(\beta_{i,l}-\alpha_{i,l})h_i$ is the heat of reaction per $gm-mole$ for the lth reaction, x_i is the mole fraction of species i, $\Delta_{ij}^{(1)}$ is defined through equation (34), and $\alpha_{i,l}$ and $\beta_{i,l}$ are the stoichiometric coefficients for reactants and products in the reaction given by equation (1). The thermal conductivities K_d given by equation (A14) and K_r given by equation (A16) are equivalent.

Similar to relations (A12) and (A13), the total specific heat at constant pressure may be defined as

$$C_p = \left[\frac{\partial h}{\partial T}\right]_p \tag{A17}$$

or, from equation (9),

$$C_p = C_{p_f} + \left[\sum_{i=1}^{11} h_i\frac{\partial C_i}{\partial T}\right]_p \tag{A18}$$

or,

$$C_p = C_{p_f} + C_{p_d} \tag{A19}$$

with

$$C_{p_d} = \left[\sum_{i=1}^{11} h_i\frac{\partial C_i}{\partial T}\right]_p \tag{A20}$$

† The formula for K_r given here already includes the effects of ambipolar diffusion (ref. 51) on the reaction conductivity of an ionized gas.

where C_{p_d} is the diffusion contribution to the specific heat at constant pressure.

Using the various definitions for the thermal conductivity and the specific heats at constant pressure, the frozen and reactive Prandtl and Lewis numbers usually employed in dimensionless heat flux calculations may now be defined.†

Generally, the frozen values of specific heat at constant pressure and thermal conductivities are employed in flowfield calculations. Associated heat flux from these calculations is, accordingly, expressed in terms of the frozen Prandtl and Lewis numbers. Alternately, one may also use total values of specific heat at constant pressure and thermal conductivity in flowfield computations. In this case, the heat flux may be expressed in terms of the reactive Prandtl and Lewis numbers. However, the total values of C_p and K as well as the reactive Prandtl and Lewis numbers can be used only with calculations involving thermal equilibrium. This is obvious from the definitions of K and C_p given by equations (A13) and (A19), respectively.

The frozen Prandtl number and Lewis numbers are defined as

$$Pr_f = C_{p_f}\mu/K_f \tag{A21}$$

$$Le_{f,i} = \rho C_{p_f} D_{ij}/K_f \tag{A22}$$

where C_{p_f} and K_f are defined by equations (9) and (37), respectively. Generally, the subscript f is not used in the literature to denote the frozen Prandtl and Lewis numbers as is done here.

The reactive Prandtl and Lewis numbers are defined by employing the total values of C_p and K as

$$Pr_r = C_p\mu/K \tag{A23}$$

$$Le_{r,i} = \rho C_p D_{ij}/K \tag{A24}$$

where C_p and K are defined through equations (A18) and (A13) or (A15), respectively. Reference 29 gives definitions of the reactive Prandtl and Lewis numbers with K defined through use of equation (A15) and employs no subscripts on Pr or Le. The frozen values defined through equations (A21) and (A22) are denoted as partial values in reference 29 and are denoted as Pr' and Le' there.

† Dr. Ken Sutton of NASA Langley Research Center provided these definitions in an unpublished memo.

Appendix B

Sample Program to Evaluate Thermodynamic Properties From Polynomial Curve-Fits

This appendix lists a sample Fortran subroutine which evaluates the species specific heats and enthalpies for an 11-species air model using polynomial curve fits as functions of temperature. Five temperature ranges are used for each species for temperatures between 300 K and 30000 K. Properties evaluated near the temperature range boundaries are smoothed by linearly averaging the polynomial coefficients to assure continuous derivatives. The subroutine may be easily modified for different needs.

```
      SUBROUTINE THERMO(T,CPI,HI)

C  Computes enthalpy and specific heat for 11 species by
C  approximating polynomials. Polynomial coefficients are stored in
C  arrays A1 to A6 and are linearly averaged at the temperature range
C  boundaries.
C
C  input: T    temperature, K
C output: CPI  specific heats of the species, cal/gm-mole-K
C         HI   enthalpies of the species, cal/gm-mole

      DIMENSION A1(11,5),A2(11,5),A3(11,5),A4(11,5),A5(11,5),A6(11,5)
      DIMENSION P(6),COEF(11,5,6)
      DIMENSION CPI(11),HI(11)

      EQUIVALENCE (A1,COEF)

C     Universal gas constant, cal/gm-mole-K
      DATA UNIR /1.987/
C
C     Coefficients are input for five temperature ranges
C
      K= 4
      L= 5
      IF(T.GT.15500.)GO TO 20
      K= 3
      L= 4
      IF(T.GT.6500)GO TO 30
      K= 2
      L= 3
      IF(T.GT.1200.)GO TO 40
      K= 1
      L= 2
      PA= 1.0
      PB= 0.0
      IF(T.LE.300.)GO TO 50
```

```
      PB= (1./400.)*(T-800.)
      PA= 1.0-PB
      GO TO 50
   40 CONTINUE
      PA= 1.0
      PB= 0.0
      IF(T.LE.5500.)GO TO 50
      PB= (1./1000.)*(T-5500.)
      PA= 1.0-PB
      GO TO 50
   20 CONTINUE
      PA= 0.0
      PB= 1.0
      IF(T.GE.25500.)GO TO 50
      PA= 1.0
      PB= 0.0
      IF(T.LE.24500.)GO TO 50
      PB= 0.001*(T-24500.)
      PA= 1.0-PB
      GO TO 50
   30 CONTINUE
      PA= 0.0
      PB= 1.0
      IF(T.GE.15500.)GO TO 50
      PA= 1.0
      PB= 0.0
      IF(T.LE.14500.)GO TO 50
      PB= 0.001*(T-14500.)
      PA= 1.0-PB
   50 CONTINUE
C
      T2= T*T
      T3= T2*T
      T4= T3*T
      TOV= 1.0/T
C     Compute properties for 11 species
      DO 65 I= 1,11
      DO 60 J= 1,6
   60 P(J)= PA*COEF(I,K,J)+ PB*COEF(I,L,J)
      HI(I)= UNIR*T*(P(1)+ 0.5*P(2)*T+ P(3)*T2/3.+ 0.25*P(4)*T3
     1 + 0.2*P(5)*T4+ P(6)*TOV)
      CPI(I)= UNIR*(P(1)+ P(2)*T+ P(3)*T2+ P(4)*T3+ P(5)*T4)
   65 CONTINUE
      RETURN
      END
```

Appendix C

Electron and Vibrational Heat Fluxes and Associated Thermal Conductivities for Flows with Thermal Nonequilibrium

Electron and vibrational heat fluxes are required in the electron energy and vibrational energy conservation equations in a multi-temperature gas model (refs. 20 and 46). The kth component of heat flux vector q_e^k resulting from the collisions between electrons only is given by

$$q_e^k = -K_e' \frac{\partial T_e}{\partial x^k} + \rho_e h_e V_e^k \tag{C1}$$

where ρ_e $(=m_e n_e)$ is the density and h_e $(=(5/2)kT_e/m_e)$ is the enthalpy of electrons, m_e is the electron mass,† n_e is the electron number density, k is Boltzmann's constant, V_e^k is the kth component of electron diffusion velocity and K_e' is the thermal conductivity of electrons resulting from collisions between electrons only. In a flowfield analysis, the diffusion velocity V_e^k is generally obtained from the electron concentration gradient by using the relation

$$V_e^k = -D_{ej} \frac{\partial \ln(C_e)}{\partial x^k} \tag{C2}$$

where D_{ej} is the binary diffusion coefficient of electrons diffusing into the species j and C_e is the electron mass fraction.

The thermal conductivity K_e' (appearing in equation (C1)) due to collisions between electrons only may be obtained from K_e (defined through equation (54)) by employing the relation

$$K_e' = K_e \left[\frac{x_e \Delta_{ee}^{(2)}(T_e)}{\sum_{j=1}^{11} x_j \Delta_{ej}^{(2)}(T_e)} \right] \tag{C3}$$

The kth component of vibrational heat flux vector q_v^k (obtained from molecule-molecule collisions only) may be written as

$$q_{vib}^k = -K_{vib}' \frac{\partial T_{vib}}{\partial x^k} + \sum_{i=\,molecules} \rho_i h_{i,vib} V_i^k \tag{C4}$$

where $h_{i,vib}$ is the vibrational component of enthalpy of the molecules, V_i^k is the kth component of diffusion velocity of the molecules, and K_{vib}' is the thermal conductivity due to the collisions between molecules only.

Referring to Fig. 2, $h_{i,vib}$ for the partially excited vibrational energy mode may be obtained from

$$[h_{i,vib}]_{T_{vib}} = [h_i]_{T_{vib}} - [(C_{p,i})_{tr} + (C_{p,i})_{rot}](T_{vib} - T_{ref}) - (\Delta h_i^f)_{T_{ref}} \tag{C5}$$

In equation (C5), the vibrational component of enthalpy for species i is obtained by using the curve-fit relation of equation (14) for the specific enthalpy h_i evaluated at temperature T_{vib} and subtracting out the contributions from the translational and rotational enthalpies evaluated at T_{vib} as well as the enthalpy of formation. Equation (C5)

† Electron mass m_e is related to the electron molecular weight M_e through the relation $m_e = M_e/N_A$, where $N_A = 6.02\times 10^{23}$ *molecules/gm−mole* is the Avogadro's number.

can be employed up to the characteristic vibrational temperature $\Theta_{i,vib}$ for the species i, i.e., for $T_{vib} \leq \Theta_{i,vib}$. For higher temperatures ($T_{vib} > \Theta_{i,vib}$), the vibrational energy mode is fully excited and $h_{i,vib}$ can be obtained from

$$[h_{i,vib}]_{T_{vib}} = R_{univ} T_{vib} / M_i \tag{C6}$$

The thermal conductivity K'_{vib} (also known as the $V-V$ thermal conductivity) in equation (C4) is obtained from the overall vibrational thermal conductivity K_{vib} (defined in equation (52)) by considering the contribution of molecule-molecule collisions only.

$$K'_{vib} = K_{vib} \sum_{i=molecules} \left[\frac{\sum_{j=molecules} x_j \Delta_{ij}^{(2)}(T_{vib})}{\sum_{j=1}^{10} x_j \Delta_{ij}^{(2)}(T_{vib}) + x_e \Delta_{ie}^{(2)}(T_e)} \right] \tag{C7}$$

Table I. Third Body Efficiences Relative to Argon

Catalytic Bodies	$Z_{(j-NS),i}$	Efficiences relative to argon of									
		O_2 i= 1	N_2 2	N 3	O 4	NO 5	NO^+ 6	O_2^+ 7	N_2^+ 8	O^+ 9	N^+ 10
M_1	1,i	9	2	25	1	1	0	0	0	0	0
M_2	2,i	1	2.5	1	0	1	0	0	0	0	0
M_3	3,i	1	1	20	20	20	0	0	0	0	0
M_4	4,i	4	1	0	0	0	0	0	0	0	0
e^-	5,i	0	0	0	0	0	1	1	1	1	1

Table II. Chemical Reactions and Rate Coefficients

No.† r	Reaction	Forward rate coefficient, $k_{f,r}$, $cm^3/mole-sec$	Backward rate coefficient, $k_{b,r}$, $cm^3/mole-sec$ or $cm^6/mole^2-sec$	Third body M
1	$O_2+M_1 \rightleftarrows 2O+M_1$	$3.61\times10^{18}T^{-1.0}exp(-5.94\times10^4/T)$	$3.01\times10^{15}T^{-0.5}$	O,N,O_2,N_2,NO
2	$N_2+M_2 \rightleftarrows 2N+M_2$	$1.92\times10^{17}T^{-0.5}exp(-1.131\times10^5/T)$	$1.09\times10^{16}T^{-0.5}$	O,O_2,N_2,NO
3	$N_2+N \rightleftarrows 2N+N$	$4.15\times10^{22}T^{-1.5}exp(-1.31\times10^5/T)$	$2.32\times10^{21}T^{-1.5}$	
4	$NO+M_3 \rightleftarrows N+O+M_3$	$3.97\times10^{20}T^{-1.5}exp(-7.56\times10^4/T)$	$1.01\times10^{20}T^{-1.5}$	O,N,O_2,N_2,NO
5	$NO+O \rightleftarrows O_2+N$	$3.18\times10^{9}T^{1.0}exp(-1.97\times10^4/T)$	$9.63\times10^{11}T^{0.5}exp(-3.6\times10^3/T)$	
6	$N_2+O \rightleftarrows NO+N$	$6.75\times10^{13}exp(-3.75\times10^4/T)$	1.5×10^{13}	
7	$N+O \rightleftarrows NO^++e^-$	$9.03\times10^{9}T^{0.5}exp(-3.24\times10^4/T)$	$1.80\times10^{19}T^{-1.0}$	
8	$O+e^- \rightleftarrows O^++e^-+e^-$	$(3.6\pm1.2)\times10^{31}T^{-2.91}exp(-1.58\times10^5/T)$	$(2.2\pm0.7)\times10^{40}T^{-4.5}$	
9	$N+e^- \rightleftarrows N^++e^-+e^-$	$(1.1\pm0.4)\times10^{32}T^{-3.14}exp(-1.69\times10^5/T)$	$(2.2\pm0.7)\times10^{40}T^{-4.5}$	
10	$O+O \rightleftarrows O_2^++e^-$	$(1.6\pm0.4)\times10^{17}T^{-0.98}exp(-8.08\times10^4/T)$	$(8.02\pm2.0)\times10^{21}T^{-1.5}$	
11	$O+O_2^+ \rightleftarrows O_2+O^+$	$2.92\times10^{18}T^{-1.11}exp(-2.8\times10^4/T)$	$7.8\times10^{11}T^{0.5}$	
12	$N_2+N^+ \rightleftarrows N+N_2^+$	$2.02\times10^{11}T^{0.81}exp(-1.3\times10^4/T)$	$7.8\times10^{11}T^{0.5}$	
13	$N+N \rightleftarrows N_2^++e^-$	$(1.4\pm0.3)\times10^{13}exp(-6.78\times10^4/T)$	$(1.5\pm0.5)\times10^{22}T^{-1.5}$	
14	$O_2+N_2 \rightleftarrows NO+NO^++e^-$	$1.38\times10^{20}T^{-1.84}exp(1.41\times10^5/T)$	$1.0\times10^{24}T^{-2.5}$	
15	$NO+M_4 \rightleftarrows NO^++e^-+M_4$	$2.2\times10^{15}T^{-0.35}exp(-1.08\times10^5/T)$	$2.2\times10^{26}T^{-2.5}$	O_2,N_2
16	$O+NO^+ \rightleftarrows NO+O^+$	$3.63\times10^{15}T^{-0.6}exp(-5.08\times10^4/T)$	1.5×10^{13}	
17	$N_2+O^+ \rightleftarrows O+N_2^+$	$3.4\times10^{19}T^{-2.0}exp(-2.3\times10^4/T)$	$2.48\times10^{19}T^{-2.2}$	
18	$N+NO^+ \rightleftarrows NO+N^+$	$1.0\times10^{19}T^{-0.93}exp(-6.1\times10^4/T)$	4.8×10^{14}	
19	$O_2+NO^+ \rightleftarrows NO+O_2$	$1.8\times10^{15}T^{0.17}exp(-3.3\times10^4/T)$	$1.8\times10^{13}T^{0.5}$	
20	$O+NO^+ \rightleftarrows O_2+N^+$	$1.34\times10^{13}T^{0.31}exp(-7.727\times10^4/T)$	1.0×10^{14}	

† Reactions and reaction rates for Nos. 1-7 are from Blottner's (ref. 13) 7-species chemical model and Nos. 8-20 are from reference 17.

Table III. Constants for Polynomial Curve-fits of Thermodynamic Properties
(300 K ≤ T ≤ 30000 K)†

Species	A_1	A_2	A_3	A_4	A_5	A_6	A_7
	0.36748E+01	-0.12081E-02	0.23240E-05	-0.63218E-09	-0.22577E-12	-0.10612E+04	0.23580E+01
	0.28963E+01	0.15155E-02	-0.57235E-06	0.99807E-10	-0.65224E-14	-0.90586E+03	0.61615E+01
N_2	0.37270E+01	0.46840E-03	-0.11400E-06	0.11540E-10	-0.32930E-15	-0.10430E+04	0.12940E+01
	0.96377E+01	-0.25728E-02	0.33020E-06	-0.14315E-10	0.20333E-15	-0.10430E+04	-0.37587E+02
	-0.51681E+01	0.23337E-02	-0.12953E-06	0.27872E-11	-0.21360E-16	-0.10430E+04	0.66217E+02
	0.36256E+01	-0.18782E-02	0.70555E-05	-0.67635E-08	0.21556E-11	-0.10475E+04	0.43053E+01
	0.36219E+01	0.73618E-03	-0.19652E-06	0.36202E-10	-0.28946E-14	-0.12020E+04	0.36151E+01
O_2	0.37210E+01	0.42540E-03	-0.28350E-07	0.60500E-12	-0.51860E-17	-0.10440E+04	0.32540E+01
	0.34867E+01	0.52384E-03	-0.39123E-07	0.10094E-11	-0.88718E-17	-0.10440E+04	0.48179E+01
	0.39620E+01	0.39446E-03	-0.29506E-07	0.73975E-12	-0.64209E-17	-0.10440E+04	0.13985E+01
	0.25031E+01	-0.21800E-04	0.54205E-07	-0.56476E-10	0.20999E-13	0.56099E+05	0.41676E+01
	0.24503E+01	0.10661E-03	-0.74653E-07	0.18797E-10	-0.10260E-14	0.56116E+05	0.44488E+01
N	0.27480E+01	-0.39090E-03	0.13380E-06	-0.11910E-10	0.33690E-15	0.56090E+05	0.28720E+01
	-0.12280E+01	0.19268E-02	-0.24370E-06	0.12193E-10	-0.19918E-15	0.56090E+05	0.28469E+02
	0.15520E+02	-0.38858E-02	0.32288E-06	-0.96053E-11	0.95472E-16	0.56090E+05	-0.88120E+02
	0.29464E+01	-0.16382E-02	0.24210E-05	-0.16028E-08	0.38907E-12	0.29148E+05	0.29640E+01
	0.25421E+01	-0.27551E-04	-0.31028E-08	0.45511E-11	-0.43680E-15	0.29231E+05	0.49203E+01
O	0.25460E+01	-0.59520E-04	0.27010E-07	-0.27980E-11	0.93800E-16	0.29150E+05	0.50490E+01
	-0.97871E-02	0.12450E-02	-0.16154E-06	0.80380E-11	-0.12624E-15	0.29150E+05	0.21711E+02
	0.16428E+02	-0.39313E-02	0.29840E-06	-0.81613E-11	0.75004E-16	0.29150E+05	-0.94358E+02
	0.40459E+01	-0.34182E-02	0.79819E-05	-0.61139E-08	0.15919E-11	0.97454E+04	0.29975E+01
	0.31890E+01	0.13382E-02	-0.52899E-06	0.95919E-10	-0.64848E-14	0.98283E+04	0.67458E+01
NO	0.38450E+01	0.25210E-03	-0.26580E-07	0.21620E-11	-0.63810E-16	0.97640E+04	0.32120E+01
	0.43309E+01	-0.58086E-04	0.28059E-07	-0.15694E-11	0.24104E-16	0.97640E+04	0.10735E+00
	0.23507E+01	0.58643E-03	-0.31316E-07	0.60495E-12	-0.40557E-17	0.97640E+04	0.14026E+02
	0.36685E+01	-0.11545E-02	0.21756E-05	-0.48227E-09	-0.27848E-12	0.11803E+06	0.31779E+01
	0.28886E+01	0.15217E-02	-0.57531E-06	0.10051E-09	-0.66044E-14	0.11819E+06	0.70027E+01
NO^+	0.22142E+01	0.17761E-02	-0.43039E-06	0.41738E-10	-0.12829E-14	0.11819E+06	0.11268E+02
	-0.33240E+01	0.24420E-02	-0.19057E-06	0.68580E-11	-0.99112E-16	0.11819E+06	0.51864E+02
	-0.43488E+01	0.24012E-02	-0.14460E-06	0.33813E-11	-0.28255E-16	0.11819E+06	0.60082E+02
	0.25000E+01	0.00000E+00	0.00000E+00	0.00000E+00	0.00000E+00	-0.74538E+03	-0.11734E+02
	0.25000E+01	0.00000E+00	0.00000E+00	0.00000E+00	0.00000E+00	-0.74538E+03	-0.11734E+02
e^-	0.25080E+01	-0.63320E-05	0.13640E-08	-0.10940E-12	0.29340E-17	-0.74500E+03	-0.12080E+02
	0.25001E+01	-0.31128E-09	0.35721E-13	-0.16037E-17	0.25071E-22	-0.74500E+03	-0.11734E+02
	0.25001E+01	0.30158E-09	-0.22620E-13	0.66734E-18	-0.68917E-23	-0.74500E+03	-0.11734E+02
	0.27270E+01	-0.28200E-03	0.11050E-06	-0.15510E-10	0.78470E-15	0.22540E+06	0.36450E+01
	0.27270E+01	-0.28200E-03	0.11050E-06	-0.15510E-10	0.78470E-15	0.22540E+06	0.36450E+01
N^+	0.24990E+01	-0.37250E-05	0.11470E-07	-0.11020E-11	0.30780E-16	0.22540E+06	0.49500E+01
	0.23856E+01	0.83495E-04	-0.58815E-08	0.18850E-12	-0.16120E-17	0.22540E+06	0.56462E+01
	0.22286E+01	0.12458E-03	-0.87636E-08	0.26204E-12	-0.21674E-17	0.22540E+06	0.67811E+01

	0.24985E+01	0.11411E-04	-0.29761E-07	0.32247E-10	-0.12376E-13	0.18795E+06	0.43864E+01
	0.25061E+01	-0.14464E-04	0.12446E-07	-0.46858E-11	0.65549E-15	0.18795E+06	0.43480E+01
O^+	0.29440E+01	-0.41080E-03	0.91560E-07	-0.58480E-11	0.11900E-15	0.18790E+06	0.17500E+01
	0.12784E+01	0.40866E-03	-0.21731E-07	0.33252E-12	0.63160E-18	0.18790E+06	0.12761E+02
	0.12889E+01	0.43343E-03	-0.26758E-07	0.62159E-12	-0.45131E-17	0.18790E+06	0.12604E+02
	0.33970E+01	0.45250E-03	0.12720E-06	-0.38790E-10	0.24590E-14	0.18260E+06	0.42050E+01
	0.33970E+01	0.45250E-03	0.12720E-06	-0.38790E-10	0.24590E-14	0.18260E+06	0.42050E+01
N_2^+	0.33780E+01	0.86290E-03	-0.12760E-06	0.80870E-11	-0.18800E-15	0.18260E+06	0.40730E+01
	0.43942E+01	0.18868E-03	-0.71272E-08	-0.17511E-12	0.67176E-17	0.18260E+06	-0.23693E+01
	0.39493E+01	0.36795E-03	-0.26910E-07	0.67110E-12	-0.58244E-17	0.18260E+06	0.65472E+00
	0.32430E+01	0.11740E-02	-0.39000E-06	0.54370E-10	-0.23920E-14	0.14000E+06	0.59250E+01
	0.32430E+01	0.11740E-02	-0.39000E-06	0.54370E-10	-0.23920E-14	0.14000E+06	0.59250E+01
O_2^+	0.51690E+01	-0.86200E-03	0.20410E-06	-0.13000E-10	0.24940E-15	0.14000E+06	-0.52960E+01
	-0.28017E+00	0.16674E-02	-0.12107E-06	0.32113E-11	-0.28349E-16	0.14000E+06	0.31013E+02
	0.20445E+01	0.10313E-02	-0.74046E-07	0.19257E-11	-0.17461E-16	0.14000E+06	0.14310E+02

† There are five rows of constants provided for each species which correspond to the following five temperature ranges, respectively.

300 K ≤ T ≤ 1000 K
1000 K ≤ T ≤ 6000 K
6000 K ≤ T ≤ 15000 K
15000 K ≤ T ≤ 25000 K
25000 K ≤ T ≤ 30000 K

For temperatures less than 300 K (which may arise in the freestream for certain flight trajectories (refs. 15,52)), the specific heats of O, O_2, N, and N_2 are practically constant. For such cases, the specific enthalpy may be obtained from the relation:

$$h_i = C_{p,i}(T - T_{ref}) + (\Delta h_i^f)_{T_{ref}}$$

with T_{ref} = 298 K and $C_{p,O}$ = 5.44 $cal/gm-mole-K$, C_{p,O_2} = 7.00 $cal/gm-mole-K$, $C_{p,N}$ = 4.97 $cal/gm-mole-K$, C_{p,N_2} = 6.96 $cal/gm-mole-K$.

Table IV. Constants for Viscosity† Curve-Fits
(1000 K ≤ T ≤ 30000 K)††

Species‡	A_{μ_i}	B_{μ_i}	C_{μ_i}	D_{μ_i}	E_{μ_i}
N_2	0.0	0.0	0.0203	0.4329	-11.8153
O_2	0.0	0.0	0.0484	-0.1455	-8.9231
N	0.0	0.0	0.0120	0.5930	-12.3805
O	0.0	0.0	0.0205	0.4257	-11.5803
NO	0.0	0.0	0.0452	-0.0609	-9.4596
NO^+	0.0913	-3.3178	45.1426	-270.3948	586.3300
e^-	0.0899	-3.2731	44.5782	-267.2522	574.4149
N^+	0.0895	-3.2573	44.3511	-265.8276	576.1313
O^+	0.0912	-3.3154	45.1290	-270.4211	586.2903
N_2^+	0.0897	-3.2618	44.4079	-266.1462	577.1449
O_2^+	0.0908	-3.3020	44.9511	-269.3877	584.4130

† Viscosity is obtained in $gm/cm-sec$

†† For temperatures less than 1000 K, Sutherland's viscosity law for air may be used for all species.

‡ The ionic species viscosities given here are for an electron pressure of 1 atm. For different electron pressures, these values should be corrected by the formula given in equation (24a) in the main text.

Table V. Constants for Frozen Thermal Conductivity† Curve-Fits
(1000 K ≤ T ≤ 30000 K)††

Species‡	$A_{K_{f,i}}$	$B_{K_{f,i}}$	$C_{K_{f,i}}$	$D_{K_{f,i}}$	$E_{K_{f,i}}$
N_2	0.0418	-1.2720	14.4571	-71.9660	122.5745
O_2	0.0776	-2.5007	30.1390	-160.1758	307.3634
N	0.0	0.0	0.0169	0.5373	-12.8682
O	0.0	0.0	0.0319	0.2485	-11.6657
NO	0.0263	-0.8130	9.4203	-47.6841	79.4139
NO^+	0.0	0.0431	-0.5477	2.1912	-17.8610
e^-	0.0908	-3.3046	44.9877	-269.6002	588.9412
N^+	0.1023	-3.6925	49.8997	-297.1291	641.3168
O^+	0.0534	-2.0710	29.9141	-188.4951	421.3914
N_2^+	0.0918	-3.3760	46.2945	-278.4425	604.2017
O_2^+	-0.0125	0.1276	2.5428	-37.7507	111.8110

† Thermal conductivity is obtained in $cal/cm-sec-K$

†† For temperatures lower than 1000 K, Sutherland's law for thermal conductivity of air may be used for each species.

‡ The ionic species frozen thermal conductivities given here are for an electron pressure of 1 atm. For different electron pressure, these values should be corrected by employing the formula given in equation (24a) in the main text.

Table VI. Constants for Diffusion Coefficient† Curve-Fits

No.††	Interaction Pair (i-j)	$A_{\bar{D}_{ij}}$	$B_{\bar{D}_{ij}}$	$C_{\bar{D}_{ij}}$	$D_{\bar{D}_{ij}}$	Temperature Range, K‡
1	N_2-N_2	0.0	0.0112	1.6182	-11.3091	
2	O_2-N_2	0.0	0.0465	0.9271	-8.1137	
3	O_2-O_2	0.0	0.0410	1.0023	-8.3597	
4	$N-N_2$	0.0	0.0195	1.4880	-10.3654	
5	$N-O_2$	0.0	0.0179	1.4848	-10.2810	
6	$N-N$	0.0	0.0033	1.5572	-11.1616	
7	$O-N_2$	0.0	0.0140	1.5824	-10.8819	
8	$O-O_2$	0.0	0.0226	1.3700	-9.6631	
9	$O-N$	0.0	-0.0048	1.9195	-11.9261	
10	$O-O$	0.0	0.0034	1.5572	-11.1729	
11	$NO-N_2$	0.0	0.0291	1.2676	-9.6878	
12	$NO-O_2$	0.0	0.0438	0.9647	-8.2380	
13	$NO-N$	0.0	0.0185	1.4882	-10.3301	
14	$NO-O$	0.0	0.0179	1.4848	-10.3155	
15	$NO-NO$	0.0	0.0364	1.1176	-8.9695	
16	NO^+-N_2	0.0	0.0	1.9000	-13.3343	
17	NO^+-O_2	0.0	0.0	1.9001	-13.3677	
18	NO^+-N	0.0	0.0	1.8999	-13.1254	
19	NO^+-O	0.0	0.0	1.9000	-13.1701	
20	NO^+-NO	0.0	0.0047	1.5552	-11.3713	
21	NO^+-NO^+	-0.1251	3.5135	-29.7280	74.1550	
22	e^--N_2	-0.1147	2.8945	-23.0085	65.9815	
23	e^--O_2	-0.0241	0.3464	0.1136	-1.3848	1000-9000
		-0.0029	0.0856	0.6655	-0.8205	9000-30000
24	e^--N	0.0	0.0	1.5000	-2.9987	
25	e^--O	0.0581	-1.5975	15.4508	-40.7370	
26	e^--NO	0.2202	-5.2261	42.0630	-106.0937	1000-8000
		0.2871	-8.3759	82.8802	-267.0227	8000-30000
27	e^--NO^+	-0.1251	3.5134	-29.7272	79.2610	
28	e^--e^-	-0.1251	3.5136	-29.7290	79.6126	
29	N^+-N_2	0.0	0.0	1.9000	-13.1144	
30	N^+-O_2	0.0	0.0	1.9000	-13.1357	
31	N^+-N	0.0	0.0033	1.5572	-11.1616	
32	N^+-O	0.0	0.0	1.9000	-13.0028	
33	N^+-NO	0.0	0.0	1.8999	-13.1254	
34	N^+-NO^+	-0.1251	3.5135	-29.7285	74.3825	
35	N^+-e^-	-0.1251	3.5134	-29.7272	79.2611	
36	N^+-N^+	-0.1251	3.5134	-29.7274	74.5342	
37	O^+-N_2	0.0	0.0	1.9000	-13.1578	
38	O^+-O_2	0.0	0.0	1.9000	-13.1810	
39	O^+-N	0.0	0.0	1.9000	-13.0028	
40	O^+-O	0.0	0.0034	1.5572	-11.1729	
41	O^+-NO	0.0	0.0	1.9000	-13.1701	
42	O^+-NO^+	-0.1251	3.5133	-29.7268	74.3330	
43	O^+-e^-	-0.1251	3.5134	-29.7274	79.2616	

44	$O^+ - N^+$	-0.1251	3.5134	-29.7275	74.5023
45	$O^+ - O^+$	-0.1251	3.5134	-29.7277	74.4687
46	$N_2^+ - N_2$	0.0	0.0	1.9000	-13.3173
47	$N_2^+ - O_2$	0.0	0.0	1.9000	-13.3495
48	$N_2^+ - N$	0.0	0.0	1.9000	-13.1144
49	$N_2^+ - O$	0.0	0.0	1.9000	-13.1578
50	$N_2^+ - NO$	0.0	0.0	1.9000	-13.3343
51	$N_2^+ - NO^+$	-0.1251	3.5134	-29.7279	74.1721
52	$N_2^+ - e^-$	-0.1251	3.5134	-29.7273	79.2613
53	$N_2^+ - N^+$	-0.1251	3.5135	-29.7288	74.3947
54	$N_2^+ - O^+$	-0.1251	3.5133	-29.7269	74.3453
55	$N_2^+ - N_2^+$	-0.1251	3.5135	-29.7282	74.1899
56	$O_2^+ - N_2$	0.0	0.0	1.9000	-13.3173
57	$O_2^+ - O_2$	0.0	0.0	1.9000	-13.3495
58	$O_2^+ - N$	0.0	0.0	1.9000	-13.1144
59	$O_2^+ - O$	0.0	0.0	1.9000	-13.1578
60	$O_2^+ - NO$	0.0	0.0	1.9000	-13.3343
61	$O_2^+ - NO^+$	-0.1251	3.5134	-29.7279	74.1721
62	$O_2^+ - e^-$	-0.1251	3.5134	-29.7273	79.2613
63	$O_2^+ - N^+$	-0.1251	3.5135	-29.7288	74.3947
64	$O_2^+ - O^+$	-0.1251	3.5133	-29.7269	74.3453
65	$O_2^+ - N_2^+$	-0.1251	3.5135	-29.7282	74.1899
66	$O_2^+ - O_2^+$	-0.1251	3.5135	-29.7282	74.1899

† Diffusion coefficients are obtained in $cm^2 - atm/sec$. Diffusion coefficients obtained from these curve-fits are for an electron pressure of 1 *atm*. For different electron pressures, the cross sections should be corrected by the formula given in the main text when the interacting pair of species are both ions or electrons or a combination of the two. Note that diffusion coefficients for N_2^+ and O_2^+ are taken to be the same.

†† Cross section Nos. 1-15 are used in a 5-species air model and Nos. 1-28 in a 7-species model.

‡ The temperature range for all curve fits is $1000 \leq T \leq 30000$ K, except where noted.

Table VII. Curve-Fit Constants for Collision Cross-Section, $\overline{\Omega}_{ij}^{(1,1)}$†

No.††	Interaction Pair (i-j)	$A_{\overline{\Omega}_{ij}^{(1,1)}}$	$B_{\overline{\Omega}_{ij}^{(1,1)}}$	$C_{\overline{\Omega}_{ij}^{(1,1)}}$	$D_{\overline{\Omega}_{ij}^{(1,1)}}$	Temperature Range, K‡
1	N_2-N_2	0.0	-0.0112	-0.1182	4.8464	
2	O_2-N_2	0.0	-0.0465	0.5729	1.6185	
3	O_2-O_2	0.0	-0.0410	0.4977	1.8302	
4	$N-N_2$	0.0	-0.0194	0.0119	4.1055	
5	$N-O_2$	0.0	-0.0179	0.0152	3.9996	
6	$N-N$	0.0	-0.0033	-0.0572	5.0452	
7	$O-N_2$	0.0	-0.0139	-0.0825	4.5785	
8	$O-O_2$	0.0	-0.0226	0.1300	3.3363	
9	$O-N$	0.0	0.0048	-0.4195	5.7774	
10	$O-O$	0.0	-0.0034	-0.0572	4.9901	
11	$NO-N_2$	0.0	-0.0291	0.2324	3.2082	
12	$NO-O_2$	0.0	-0.0438	0.5352	1.7252	
13	$NO-N$	0.0	-0.0185	0.0118	4.0590	
14	$NO-O$	0.0	-0.0179	0.0152	3.9996	
15	$NO-NO$	0.0	-0.0364	0.3825	2.4718	
16	NO^+-N_2	0.0	0.0	-0.4000	6.8543	
17	NO^+-O_2	0.0	0.0	-0.4000	6.8543	
18	NO^+-N	0.0	0.0	-0.4000	6.8543	
19	NO^+-O	0.0	0.0	-0.4000	6.8543	
20	NO^+-NO	0.0	-0.0047	-0.0551	4.8737	
21	NO^+-NO^+	0.1251	-3.5134	31.2277	-80.6515	
22	e^--N_2	0.1147	-2.8945	24.5080	-67.3691	
23	e^--O_2	0.0241	-0.3467	1.3887	-0.0110	1000-9000
		0.0025	-0.0742	0.7235	-0.2116	9000-30000
24	e^--N	0.0	0.0	0.0	1.6094	
25	e^--O	0.0164	-0.2431	1.1231	-1.5561	1000-9000
		-0.2027	5.6428	-51.5646	155.6091	9000-30000
26	e^--NO	-0.2202	5.2265	-40.5659	104.7126	1000-8000
		-0.2871	8.3757	-81.3787	265.6292	8000-30000
27	e^--NO^+	0.1251	-3.5134	31.2277	-80.6515	
28	e^--e^-	0.1251	-3.5134	31.2277	-80.6515	
29	N^+-N_2	0.0	0.0	-0.4000	6.8543	
30	N^+-O_2	0.0	0.0	-0.4000	6.8543	
31	N^+-N	0.0	-0.0033	-0.0572	5.0452	
32	N^+-O	0.0	0.0	-0.4000	6.8543	
33	N^+-NO	0.0	0.0	-0.4000	6.8543	
34	N^+-NO^+	0.1251	-3.5134	31.2277	-80.6515	
35	N^+-e^-	0.1251	-3.5134	31.2277	-80.6515	
36	N^+-N^+	0.1251	-3.5134	31.2277	-80.6515	
37	O^+-N_2	0.0	0.0	-0.4000	6.8543	
38	O^+-O_2	0.0	0.0	-0.4000	6.8543	
39	O^+-N	0.0	0.0	-0.4000	6.8543	
40	O^+-O	0.0	-0.0034	-0.0572	4.9901	
41	O^+-NO	0.0	0.0	-0.4000	6.8543	
42	O^+-NO^+	0.1251	-3.5134	31.2277	-80.6515	

43	$O^+ - e^-$	0.1251	-3.5134	31.2277	-80.6515
44	$O^+ - N^+$	0.1251	-3.5134	31.2277	-80.6515
45	$O^+ - O^+$	0.1251	-3.5134	31.2277	-80.6515
46	$N_2^+ - N_2$	0.0	0.0	-0.4000	6.8543
47	$N_2^+ - O_2$	0.0	0.0	-0.4000	6.8543
48	$N_2^+ - N$	0.0	0.0	-0.4000	6.8543
49	$N_2^+ - O$	0.0	0.0	-0.4000	6.8543
50	$N_2^+ - NO$	0.0	0.0	-0.4000	6.8543
51	$N_2^+ - NO^+$	0.1251	-3.5134	31.2277	-80.6515
52	$N_2^+ - e^-$	0.1251	-3.5134	31.2277	-80.6515
53	$N_2^+ - N^+$	0.1251	-3.5134	31.2277	-80.6515
54	$N_2^+ - O^+$	0.1251	-3.5134	31.2277	-80.6515
55	$N_2^+ - N_2^+$	0.1251	-3.5134	31.2277	-80.6515
56	$O_2^+ - N_2$	0.0	0.0	-0.4000	6.8543
57	$O_2^+ - O_2$	0.0	0.0	-0.4000	6.8543
58	$O_2^+ - N$	0.0	0.0	-0.4000	6.8543
59	$O_2^+ - O$	0.0	0.0	-0.4000	6.8543
60	$O_2^+ - NO$	0.0	0.0	-0.4000	6.8543
61	$O_2^+ - NO^+$	0.1251	-3.5134	31.2277	-80.6515
62	$O_2^+ - e^-$	0.1251	-3.5134	31.2277	-80.6515
63	$O_2^+ - N^+$	0.1251	-3.5134	31.2277	-80.6515
64	$O_2^+ - O^+$	0.1251	-3.5134	31.2277	-80.6515
65	$O_2^+ - N_2^+$	0.1251	-3.5134	31.2277	-80.6515
66	$O_2^+ - O_2^+$	0.1251	-3.5134	31.2277	-80.6515

† Cross sections are obtained in Å^2; $1\ \text{Å}^2 = 10^{-16} cm^2$. Collision cross sections obtained from these curve-fits are for an electron pressure of 1 *atm*. For different electron pressures, the cross sections should be corrected by the formula given in the main text when the interacting pair of species are both ions or electrons or a combination of the two. Note that cross sections for N_2^+ and O_2^+ are taken to be the same.

†† Cross section Nos. 1-15 are used in a 5-species air model and Nos. 1-28 in a 7-species model.

‡ The temperature range for all curve fits is $1000 \leq T \leq 30000$ K, except where noted.

Table VIII. Curve-Fit Constants for Collision Cross-Section, $\overline{\Omega}_{ij}^{(2,2)}$†

No.††	Interaction Pair (i-j)	$A_{\overline{\Omega}_{ij}^{(2,2)}}$	$B_{\overline{\Omega}_{ij}^{(2,2)}}$	$C_{\overline{\Omega}_{ij}^{(2,2)}}$	$D_{\overline{\Omega}_{ij}^{(2,2)}}$	Temperature Range, K‡
1	N_2-N_2	0.0	-0.0203	0.0683	4.0900	
2	O_2-N_2	0.0	-0.0558	0.7590	0.8955	
3	O_2-O_2	0.0	-0.0485	0.6475	1.2607	
4	$N-N_2$	0.0	-0.0190	0.0239	4.1782	
5	$N-O_2$	0.0	-0.0203	0.0730	3.8818	
6	$N-N$	0.0	-0.0118	-0.0960	4.3252	
7	$O-N_2$	0.0	-0.0169	-0.0143	4.4195	
8	$O-O_2$	0.0	-0.0247	0.1783	3.2517	
9	$O-N$	0.0	0.0065	-0.4467	6.0426	
10	$O-O$	0.0	-0.0207	0.0780	3.5658	
11	$NO-N_2$	0.0	-0.0385	0.4226	2.4507	
12	$NO-O_2$	0.0	-0.0522	0.7045	1.0738	
13	$NO-N$	0.0	-0.0196	0.0478	4.0321	
14	$NO-O$	0.0	-0.0203	0.0730	3.8818	
15	$NO-NO$	0.0	-0.0453	0.5624	1.7669	
16	NO^+-N_2	0.0	0.0	-0.4000	6.7760	
17	NO^+-O_2	0.0	0.0	-0.4000	6.7760	
18	NO^+-N	0.0	0.0	-0.4000	6.7760	
19	NO^+-O	0.0	0.0	-0.4000	6.7760	
20	NO^+-NO	0.0	0.0	-0.4000	6.7760	
21	NO^+-NO^+	0.1251	-3.5135	31.2281	-80.1163	
22	e^--N_2	0.1147	-2.8945	24.5080	-67.3691	
23	e^--O_2	0.0241	-0.3467	1.3887	-0.0110	1000-9000
		0.0025	-0.0742	0.7235	-0.2116	9000-30000
24	e^--N	0.0	0.0	0.0	1.6094	
25	e^--O	0.0164	-0.2431	1.1231	-1.5561	1000-9000
		-0.2027	5.6428	-51.5646	155.6091	9000-30000
26	e^--NO	-0.2202	5.2265	-40.5659	104.7126	1000-8000
		-0.2871	8.3757	-81.3787	265.6292	8000-30000
27	e^--NO^+	0.1251	-3.5134	31.2274	-80.1684	
28	e^--e^-	0.1251	-3.5134	31.2274	-80.1684	
29	N^+-N_2	0.0	0.0	-0.4000	6.7760	
30	N^+-O_2	0.0	0.0	-0.4000	6.7760	
31	N^+-N	0.0	0.0	-0.4146	6.9078	
32	N^+-O	0.0	0.0	-0.4000	6.7760	
33	N^+-NO	0.0	0.0	-0.4000	6.7760	
34	N^+-NO^+	0.1251	-3.5135	31.2281	-80.1163	
35	N^+-e^-	0.1251	-3.5134	31.2274	-80.1684	
36	N^+-N^+	0.1251	-3.5135	31.2281	-80.1163	
37	O^+-N_2	0.0	0.0	-0.4000	6.7760	
38	O^+-O_2	0.0	0.0	-0.4000	6.7760	
39	O^+-N	0.0	0.0	-0.4000	6.7760	
40	O^+-O	0.0	0.0	-0.4235	6.7787	
41	O^+-NO	0.0	0.0	-0.4000	6.7760	
42	O^+-NO^+	0.1251	-3.5135	31.2281	-80.1163	

43	$O^+ - e^-$	0.1251	-3.5134	31.2274	-80.1684
44	$O^+ - N^+$	0.1251	-3.5135	31.2281	-80.1163
45	$O^+ - O^+$	0.1251	-3.5135	31.2281	-80.1163
46	$N_2^+ - N_2$	0.0	0.0	-0.4000	6.7760
47	$N_2^+ - O_2$	0.0	0.0	-0.4000	6.7760
48	$N_2^+ - N$	0.0	0.0	-0.4000	6.7760
49	$N_2^+ - O$	0.0	0.0	-0.4000	6.7760
50	$N_2^+ - NO$	0.0	0.0	-0.4000	6.7760
51	$N_2^+ - NO^+$	0.1251	-3.5135	31.2281	-80.1163
52	$N_2^+ - e^-$	0.1251	-3.5134	31.2274	-80.1684
53	$N_2^+ - N^+$	0.1251	-3.5135	31.2281	-80.1163
54	$N_2^+ - O^+$	0.1251	-3.5135	31.2281	-80.1163
55	$N_2^+ - N_2^+$	0.1251	-3.5135	31.2281	-80.1163
56	$O_2^+ - N_2$	0.0	0.0	-0.4000	6.7760
57	$O_2^+ - O_2$	0.0	0.0	-0.4000	6.7760
58	$O_2^+ - N$	0.0	0.0	-0.4000	6.7760
59	$O_2^+ - O$	0.0	0.0	-0.4000	6.7760
60	$O_2^+ - NO$	0.0	0.0	-0.4000	6.7760
61	$O_2^+ - NO^+$	0.1251	-3.5135	31.2281	-80.1163
62	$O_2^+ - e^-$	0.1251	-3.5135	31.2281	-80.1163
63	$O_2^+ - N^+$	0.1251	-3.5135	31.2281	-80.1163
64	$O_2^+ - O^+$	0.1251	-3.5135	31.2281	-80.1163
65	$O_2^+ - N_2^+$	0.1251	-3.5135	31.2281	-80.1163
66	$O_2^+ - O_2^+$	0.1251	-3.5135	31.2281	-80.1163

† Cross sections are obtained in Å^2; $1\,\text{Å}^2 = 10^{-16} cm^2$. Collision cross sections obtained from these curve-fits are for an electron pressure of 1 *atm*. For different electron pressures, the cross sections should be corrected by the formula given in the main text when the interacting pair of species are both ions or electrons or a combination of the two. Note that cross sections for N_2^+ and O_2^+ are taken to be the same.

†† Cross section Nos. 1-15 are used in a 5-species air model and Nos. 1-28 in a 7-species model.

‡ The temperature range for all curve fits is $1000 \leq T \leq 30000$ K, except where noted.

Table IX. Curve-Fit Constants for Collision Cross-Section Ratio, B_{ij}^{*}†
(1000 K≤ T ≤ 30000 K)

No.††	Interaction Pair (i-j)	$A_{B_{ij}^{*}}$	$B_{B_{ij}^{*}}$	$C_{B_{ij}^{*}}$	$D_{B_{ij}^{*}}$
1	$N_2 - N_2$	0.0	-0.0073	0.1444	-0.5625
2	$O_2 - N_2$	0.0	-0.0019	0.0602	-0.2175
3	$O_2 - O_2$	0.0	0.0001	0.0181	-0.0306
4	$N - N_2$	0.0	0.0043	-0.0494	0.2850
5	$N - O_2$	0.0	0.0033	-0.0366	0.2332
6	$N - N$	0.0	0.0002	0.0002	0.0537
7	$O - N_2$	0.0	0.0042	-0.0471	0.2747
8	$O - O_2$	0.0	0.0024	-0.0245	0.1808
9	$O - N$	0.0	0.0147	-0.2628	1.2943
10	$O - O$	0.0	0.0002	0.0	0.0549
11	$NO - N_2$	0.0	-0.0045	0.1010	-0.3872
12	$NO - O_2$	0.0	-0.0010	0.0410	-0.1312
13	$NO - N$	0.0	0.0038	-0.0425	0.2574
14	$NO - O$	0.0	0.0033	-0.0366	0.2332
15	$NO - NO$	0.0	-0.0027	0.0700	-0.2553
16	$NO^+ - N_2$	0.0	0.0	0.0	0.1933
17	$NO^+ - O_2$	0.0	0.0	0.0	0.1933
18	$NO^+ - N$	0.0	0.0	0.0	0.1933
19	$NO^+ - O$	0.0	0.0	0.0	0.1933
20	$NO^+ - NO$	0.0	0.0003	-0.0006	0.0632
21	$NO^+ - NO^+$	0.0	0.0	0.0	0.4463
22	$e^- - N_2$	0.0	0.0	0.0	0.0
23	$e^- - O_2$	0.0	0.0	0.0	0.0
24	$e^- - N$	0.0	0.0	0.0	0.0
25	$e^- - O$	0.0	0.0	0.0	0.0
26	$e^- - NO$	0.0	0.0	0.0	0.0
27	$e^- - NO^+$	0.0	0.0	0.0	0.4463
28	$e^- - e^-$	0.0	0.0	0.0	0.4463
29	$N^+ - N_2$	0.0	0.0	0.0	0.1933
30	$N^+ - O_2$	0.0	0.0	0.0	0.1933
31	$N^+ - N$	0.0	0.0002	0.0002	0.0537
32	$N^+ - O$	0.0	0.0	0.0	0.1933
33	$N^+ - NO$	0.0	0.0	0.0	0.1933
34	$N^+ - NO^+$	0.0	0.0	0.0	0.4463
35	$N^+ - e^-$	0.0	0.0	0.0	0.4463
36	$N^+ - N^+$	0.0	0.0	0.0	0.4463
37	$O^+ - N_2$	0.0	0.0	0.0	0.1933
38	$O^+ - O_2$	0.0	0.0	0.0	0.1933
39	$O^+ - N$	0.0	0.0	0.0	0.1933
40	$O^+ - O$	0.0	0.0002	0.0	0.0549
41	$O^- - NO$	0.0	0.0	0.0	0.1933
42	$O^+ - NO^+$	0.0	0.0	0.0	0.4463
43	$O^+ - e^-$	0.0	0.0	0.0	0.4463
44	$O^+ - N^+$	0.0	0.0	0.0	0.4463

45	$O^+ - O^+$	0.0	0.0	0.0	0.4463
46	$N_2^+ - N_2$	0.0	0.0	0.0	0.1933
47	$N_2^+ - O_2$	0.0	0.0	0.0	0.1933
48	$N_2^+ - N$	0.0	0.0	0.0	0.1933
49	$N_2^+ - O$	0.0	0.0	0.0	0.1933
50	$N_2^+ - NO$	0.0	0.0	0.0	0.1933
51	$N_2^+ - NO^+$	0.0	0.0	0.0	0.4463
52	$N_2^+ - e^-$	0.0	0.0	0.0	0.4463
53	$N_2^+ - N^+$	0.0	0.0	0.0	0.4463
54	$N_2^+ - O^+$	0.0	0.0	0.0	0.4463
55	$N_2^+ - N_2^+$	0.0	0.0	0.0	0.4463
56	$O_2^+ - N_2$	0.0	0.0	0.0	0.1933
57	$O_2^+ - O_2$	0.0	0.0	0.0	0.1933
58	$O_2^+ - N$	0.0	0.0	0.0	0.1933
59	$O_2^+ - O$	0.0	0.0	0.0	0.1933
60	$O_2^+ - NO$	0.0	0.0	0.0	0.1933
61	$O_2^+ - NO^+$	0.0	0.0	0.0	0.4463
62	$O_2^+ - e^-$	0.0	0.0	0.0	0.4463
63	$O_2^+ - N^+$	0.0	0.0	0.0	0.4463
64	$O_2^+ - O^+$	0.0	0.0	0.0	0.4463
65	$O_2^+ - N_2^+$	0.0	0.0	0.0	0.4463
66	$O_2^+ - O_2^+$	0.0	0.0	0.0	0.4463

† The collision cross section ratios are dimensionless parameters and are valid as given for all electron pressures.

†† Cross section Nos. 1-15 are used in a 5-species air model and Nos. 1-28 in a 7-species model.

Regions with chemical and thermal nonequilibrium	
Region	Aerothermal phenomenon
Ⓐ	Chemical and thermal equilibrium
Ⓑ	Chemical nonequilibrium with thermal equilibrium
Ⓒ	Chemical and thermal nonequilibrium

Chemical species in high temperature air		
Region	Air chemical model	Species present
Ⅰ	2 species	O_2, N_2
Ⅱ	5 species	O_2, N_2, O, N, NO
Ⅲ	7 species	$O_2, N_2, O, N, NO, NO^+, e^-$
Ⅳ	11 species	$O_2, N_2, O, N, NO, O_2^+, N_2^+, O^+, N^+, NO^+, e^-$

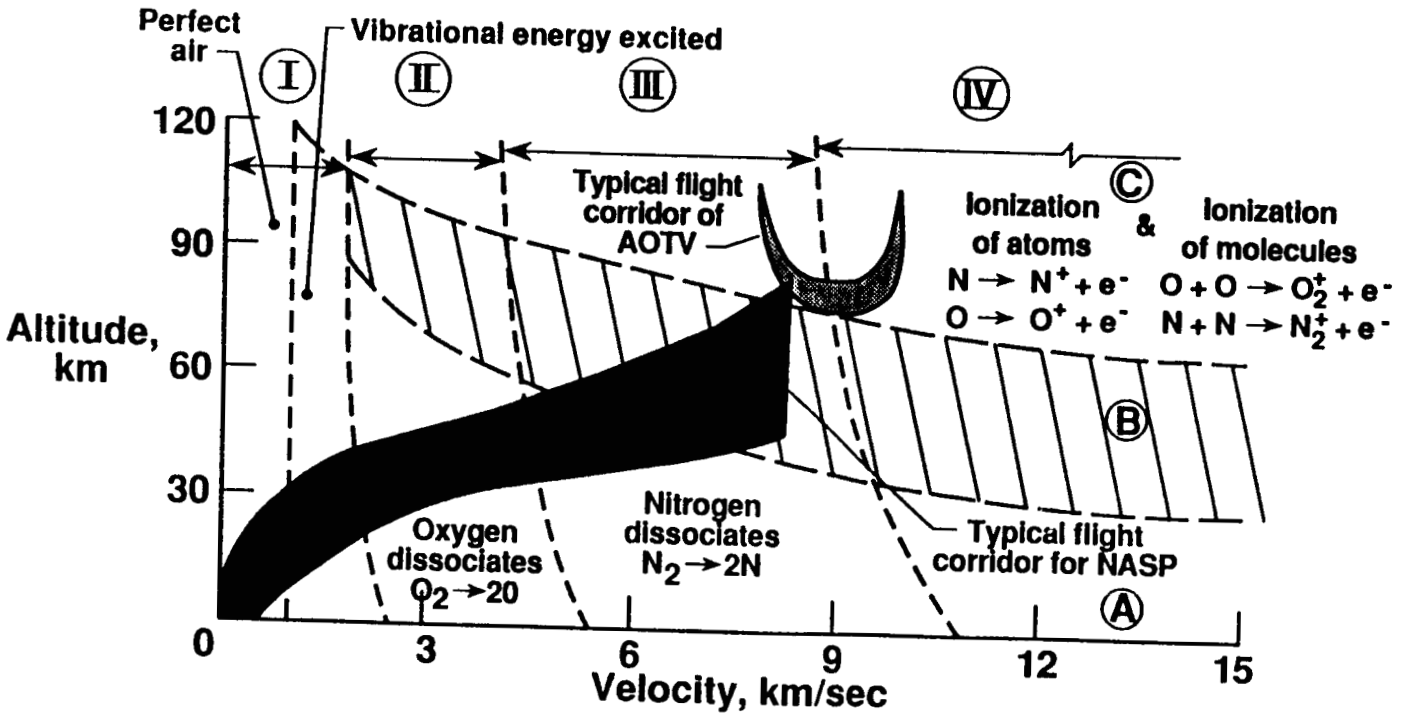

Figure 1. Flight stagnation region air chemistry (adapted from ref. 5).

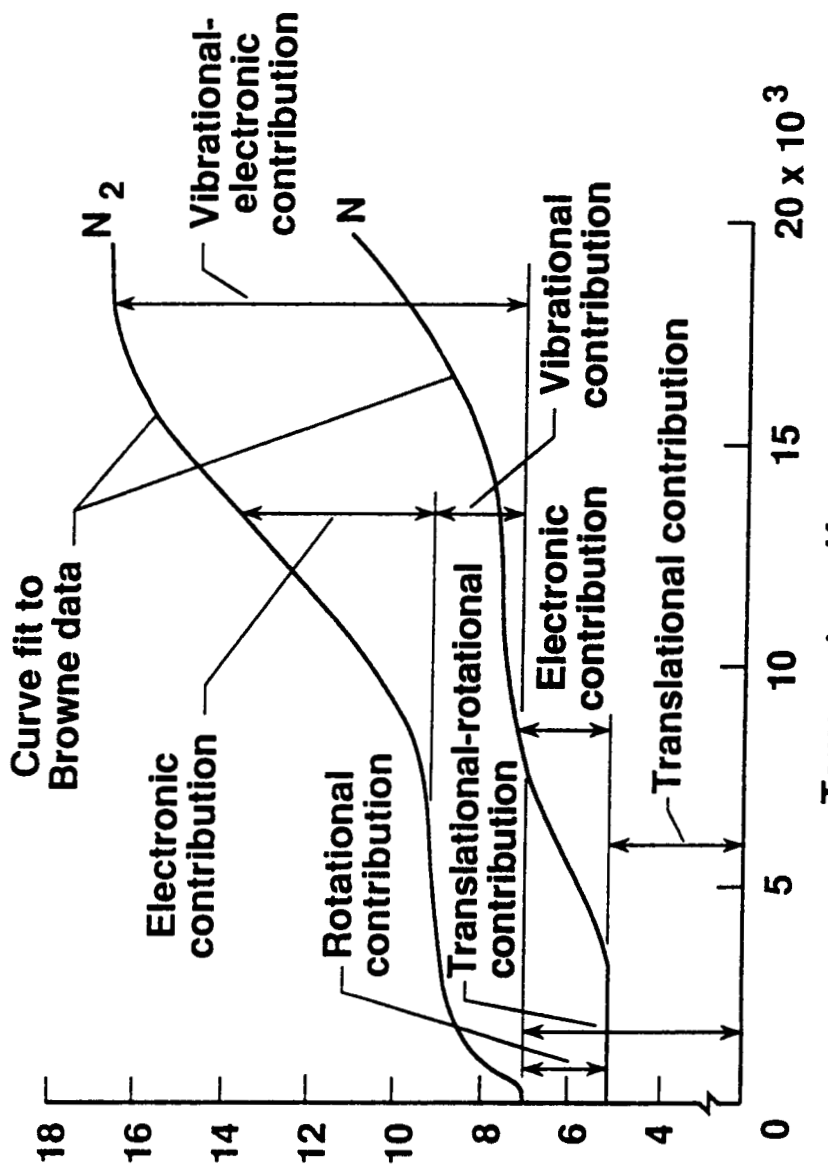

Figure 2. Specific heats of monatomic and diatomic nitrogen with contributions from the excitation of different energy modes.

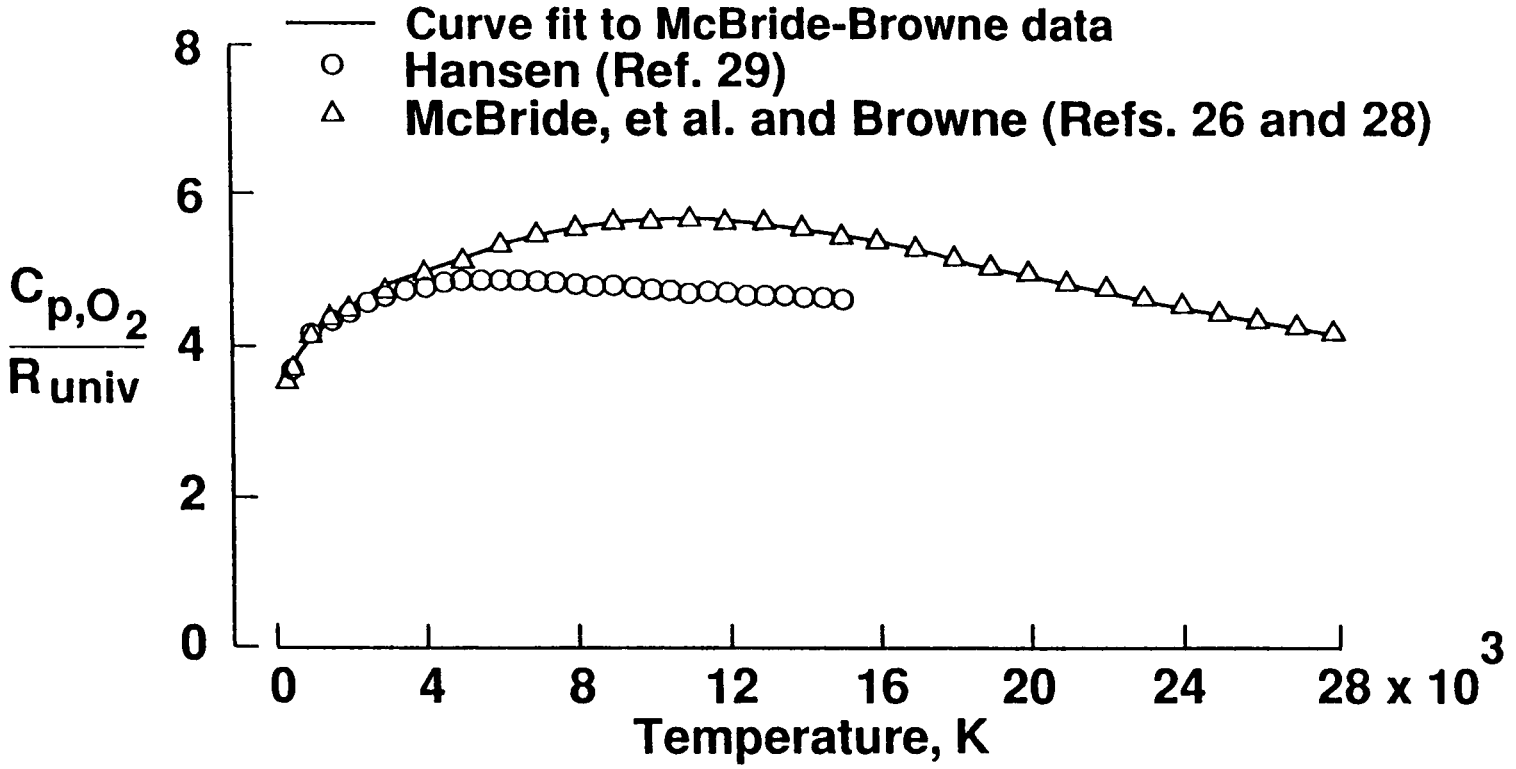

(a) Diatomic oxygen.

Figure 3. Curve fit to the specific heat values obtained by McBride et al. (ref. 26) and Browne (ref. 28) and comparison with Hansen's values (ref. 29).

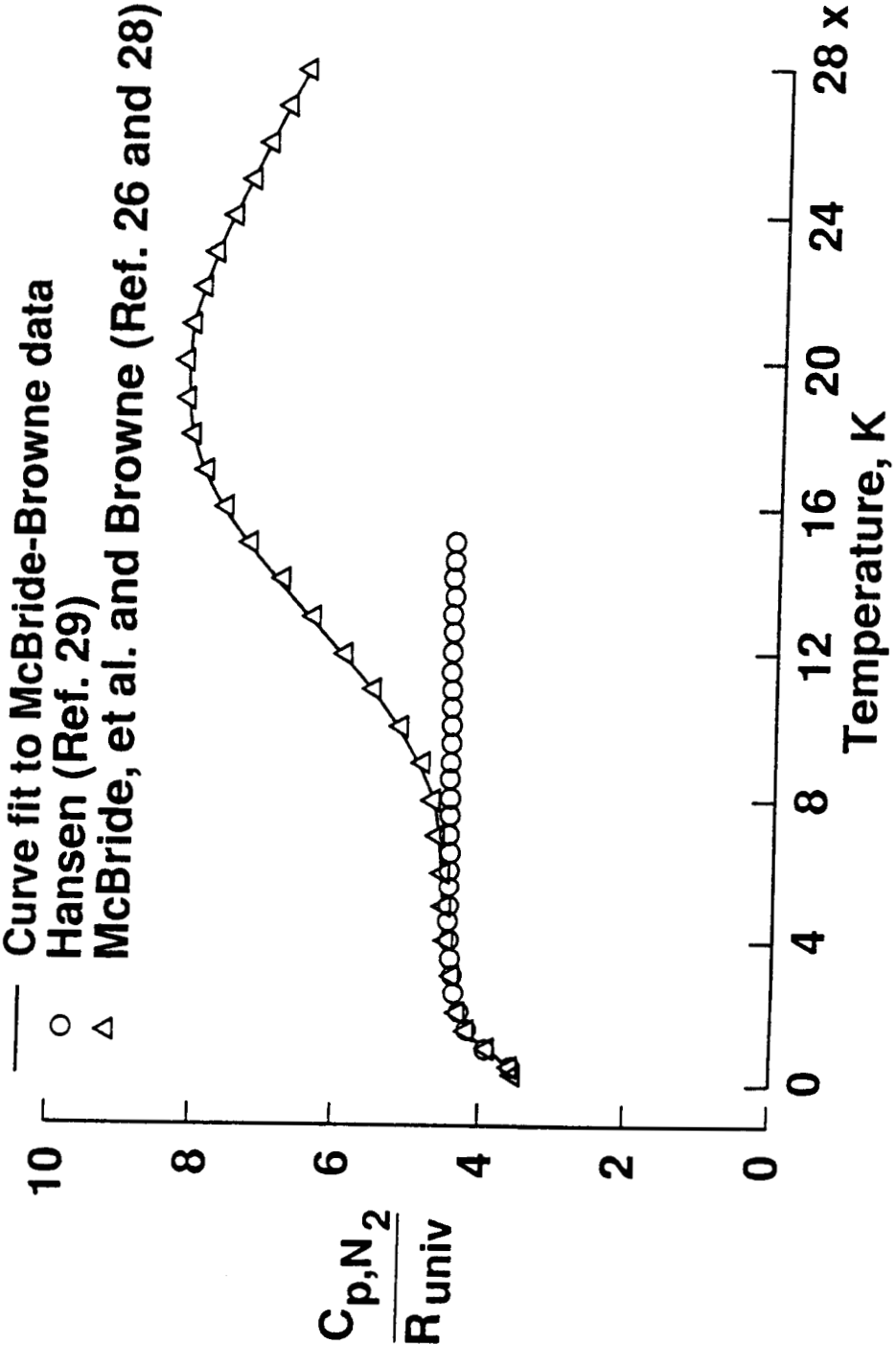

(b) Diatomic nitrogen.

Figure 3. Continued.

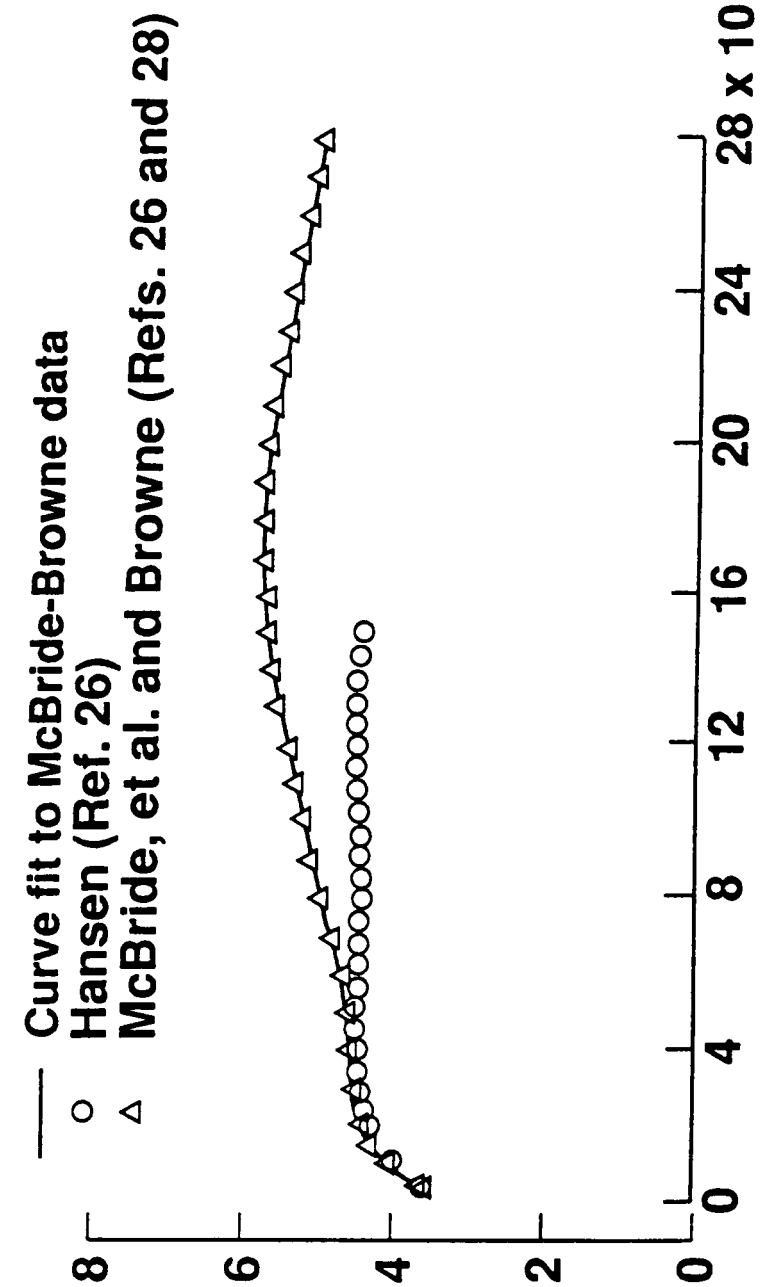

(c) Nitric oxide.

Figure 3. Concluded.

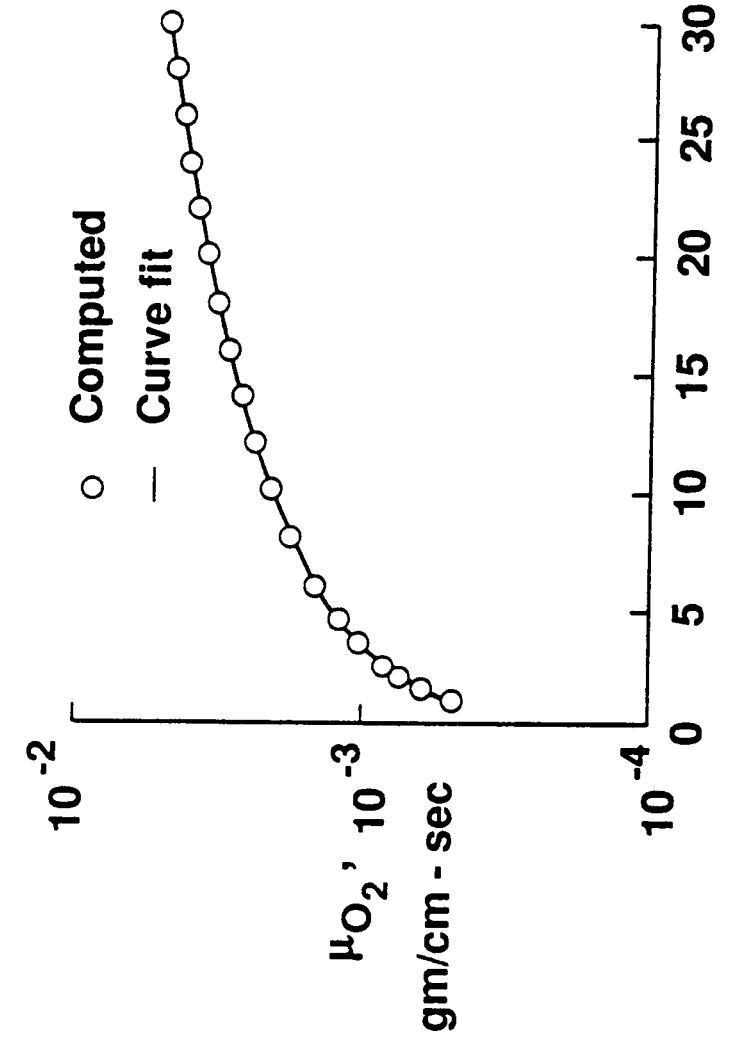

(a) Diatomic oxygen.

Figure 4. Curve fit to the viscosity values obtained by employing the collision cross sections based on the data of Yos (ref. 32).

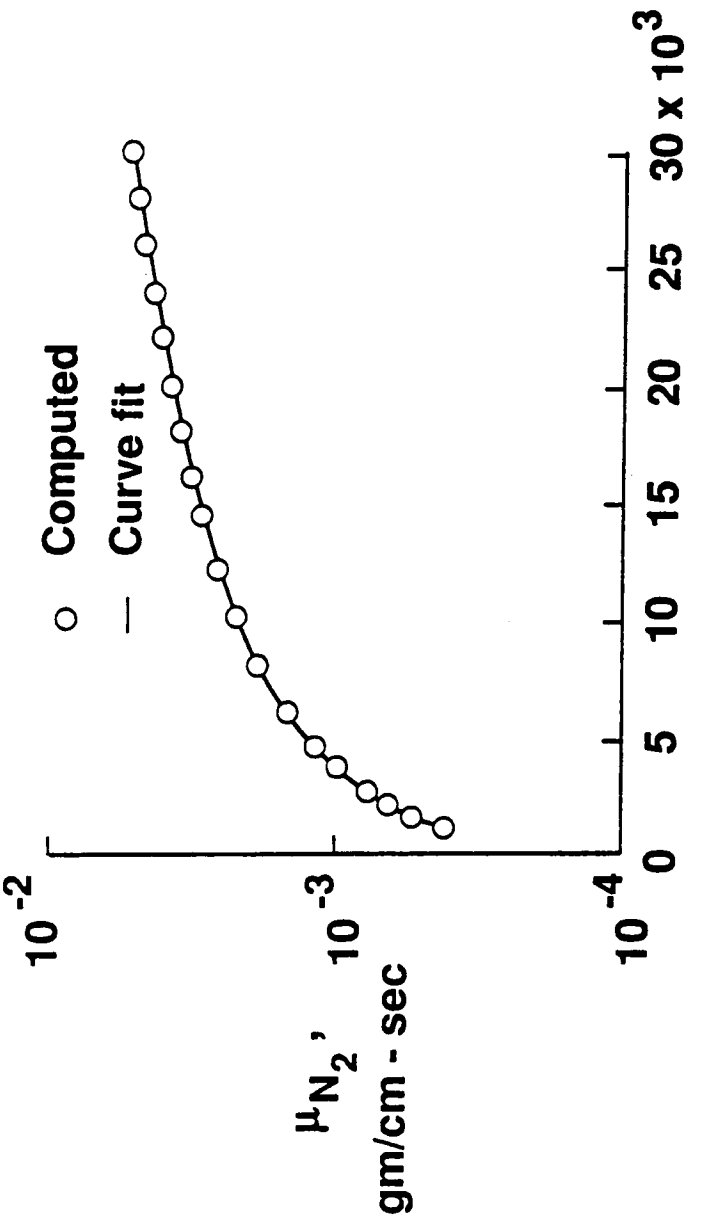

(b) Diatomic nitrogen.

Figure 4. Continued.

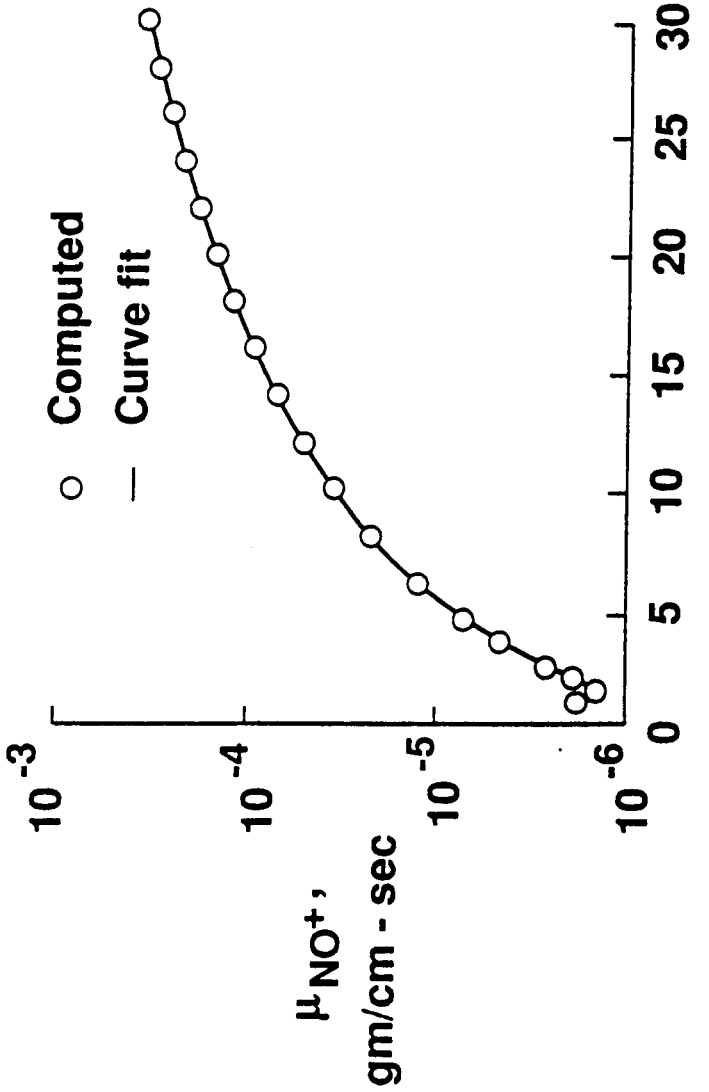

(c) Ionized nitric oxide.

Figure 4. Continued.

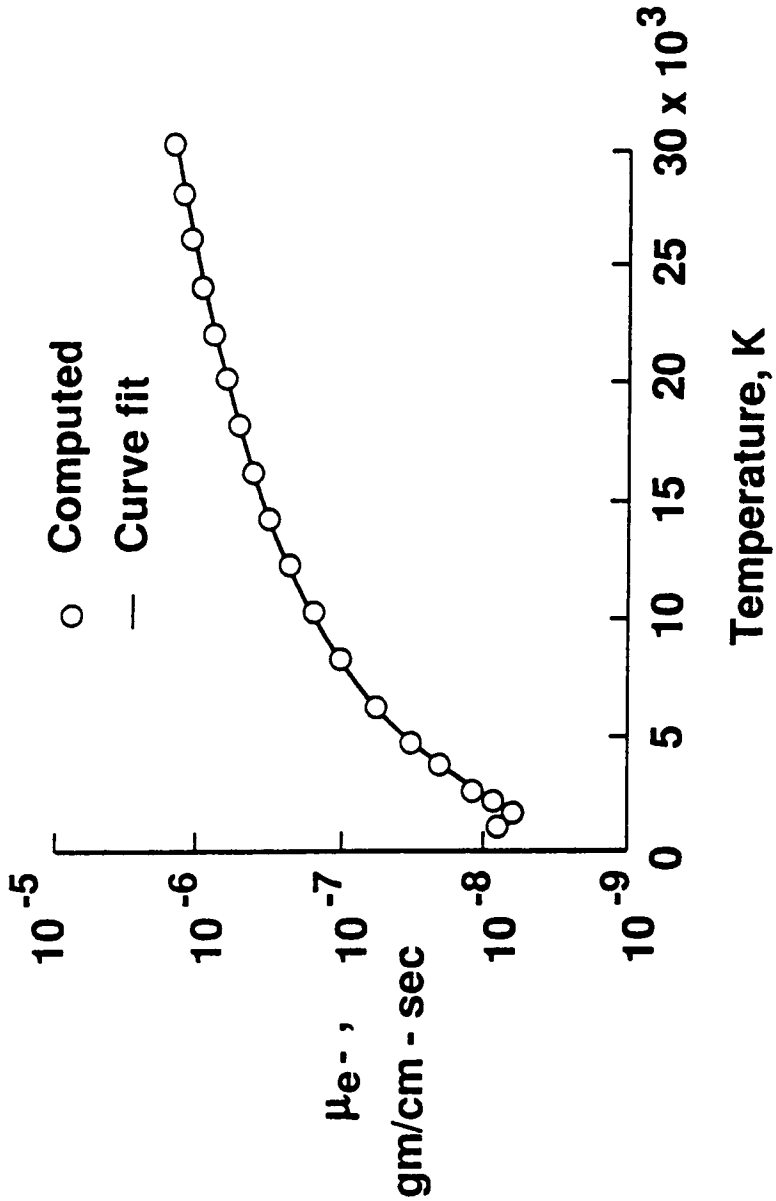

(d) Electron.

Figure 4. Concluded.

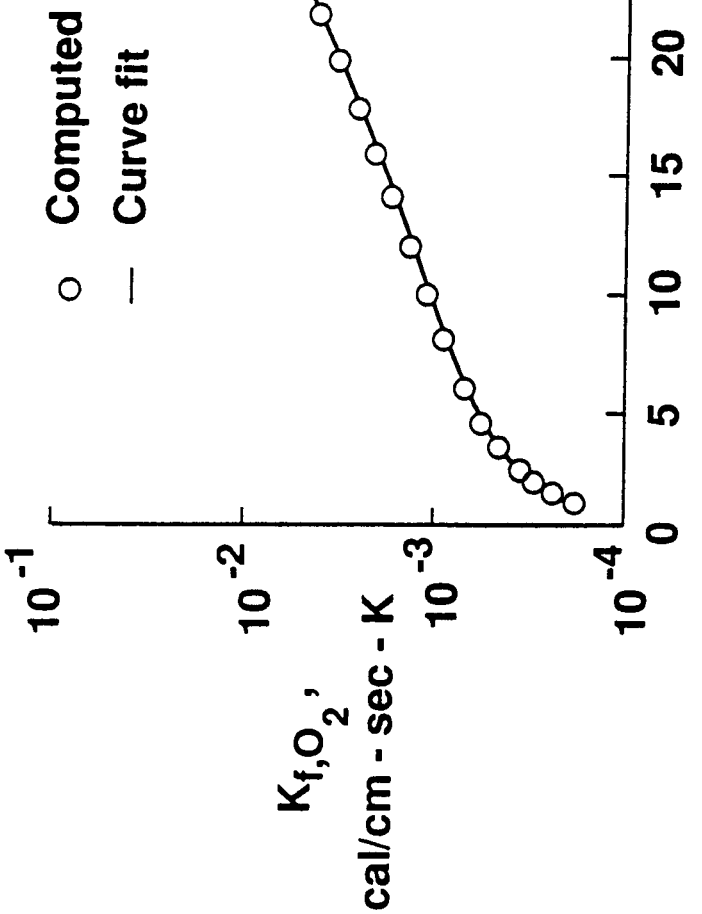

(a) Diatomic oxygen.

Figure 5. Curve fit to the frozen thermal conductivity values obtained by employing the collision cross sections based on the data of Yos (ref. 32).

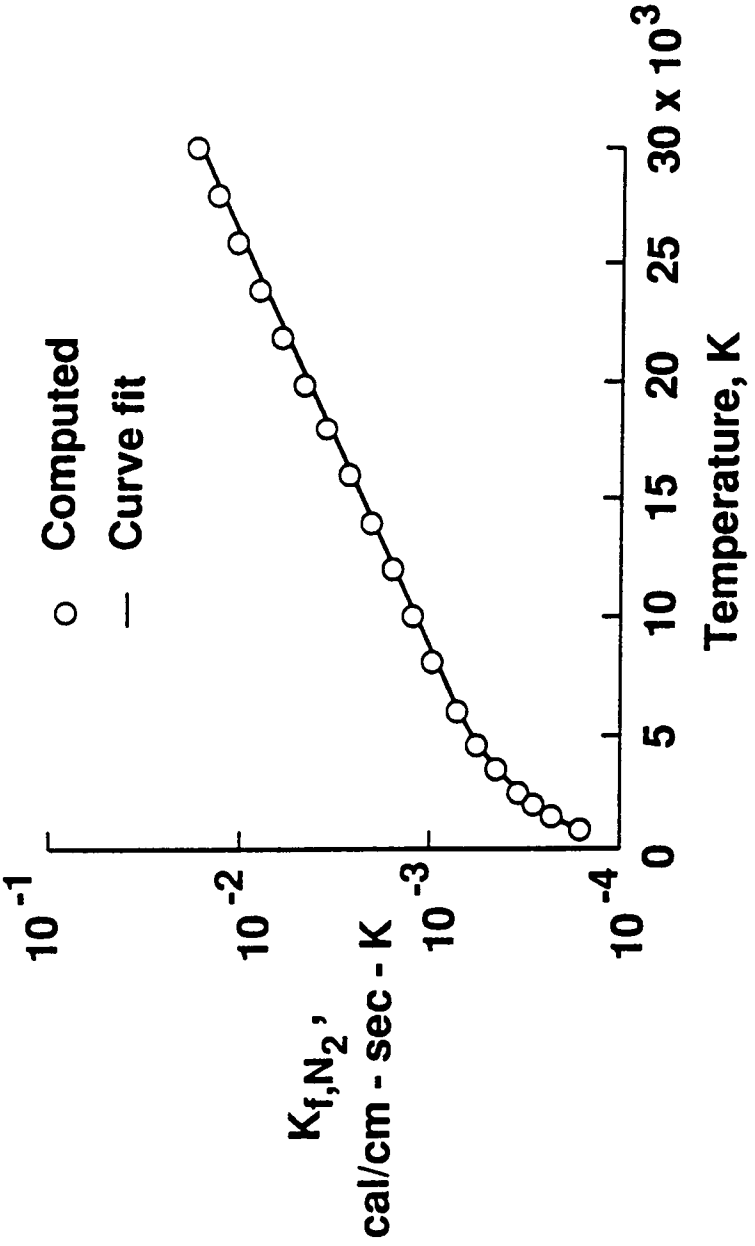

(b) Diatomic nitrogen.

Figure 5. Continued.

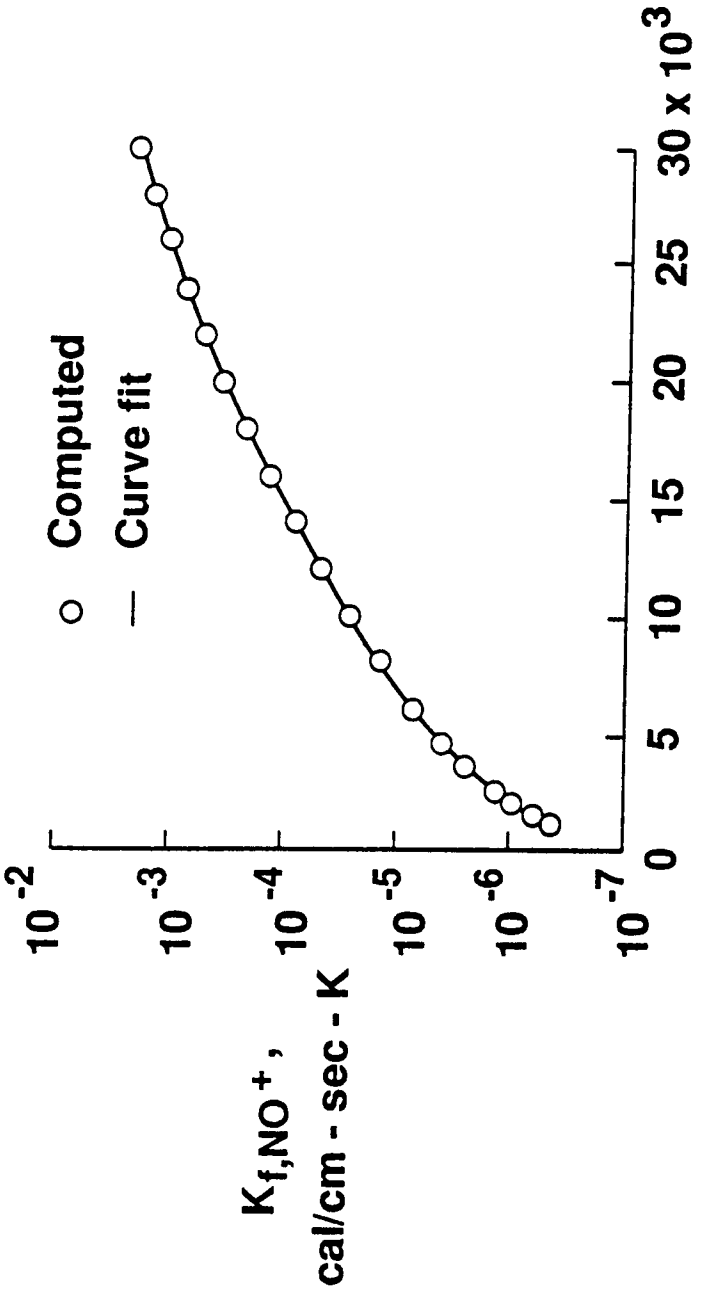

(c) Ionized nitric oxide.

Figure 5. Continued.

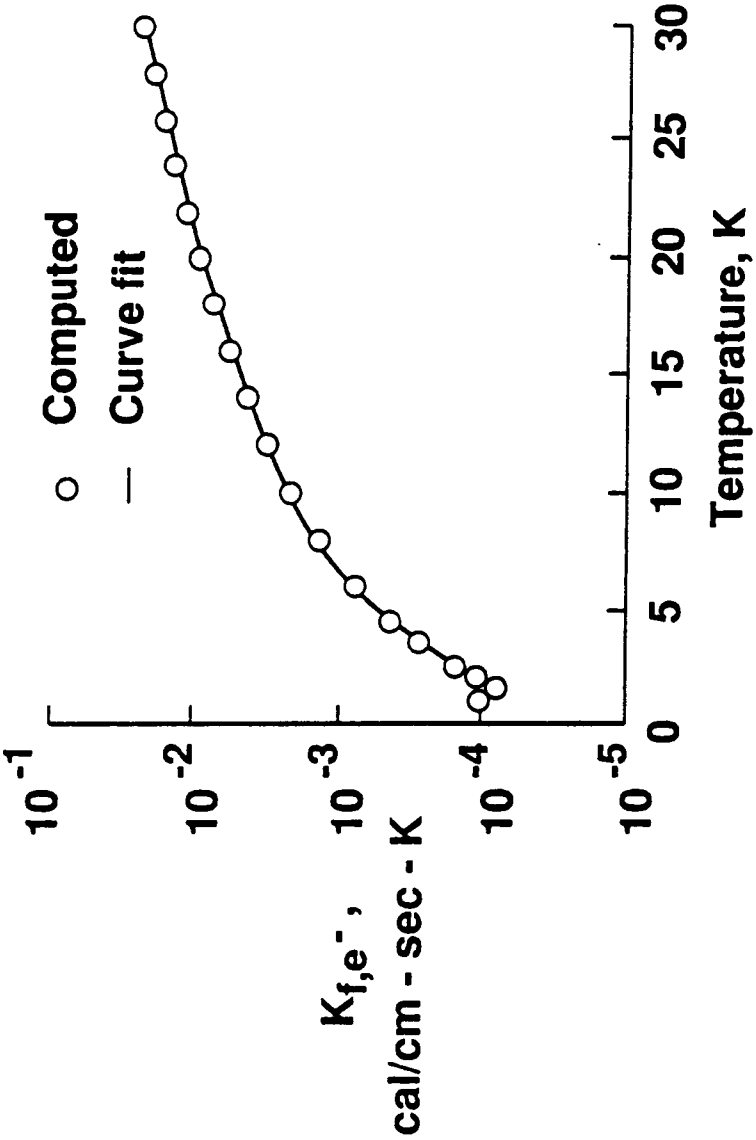

(d) Electron.

Figure 5. Concluded.

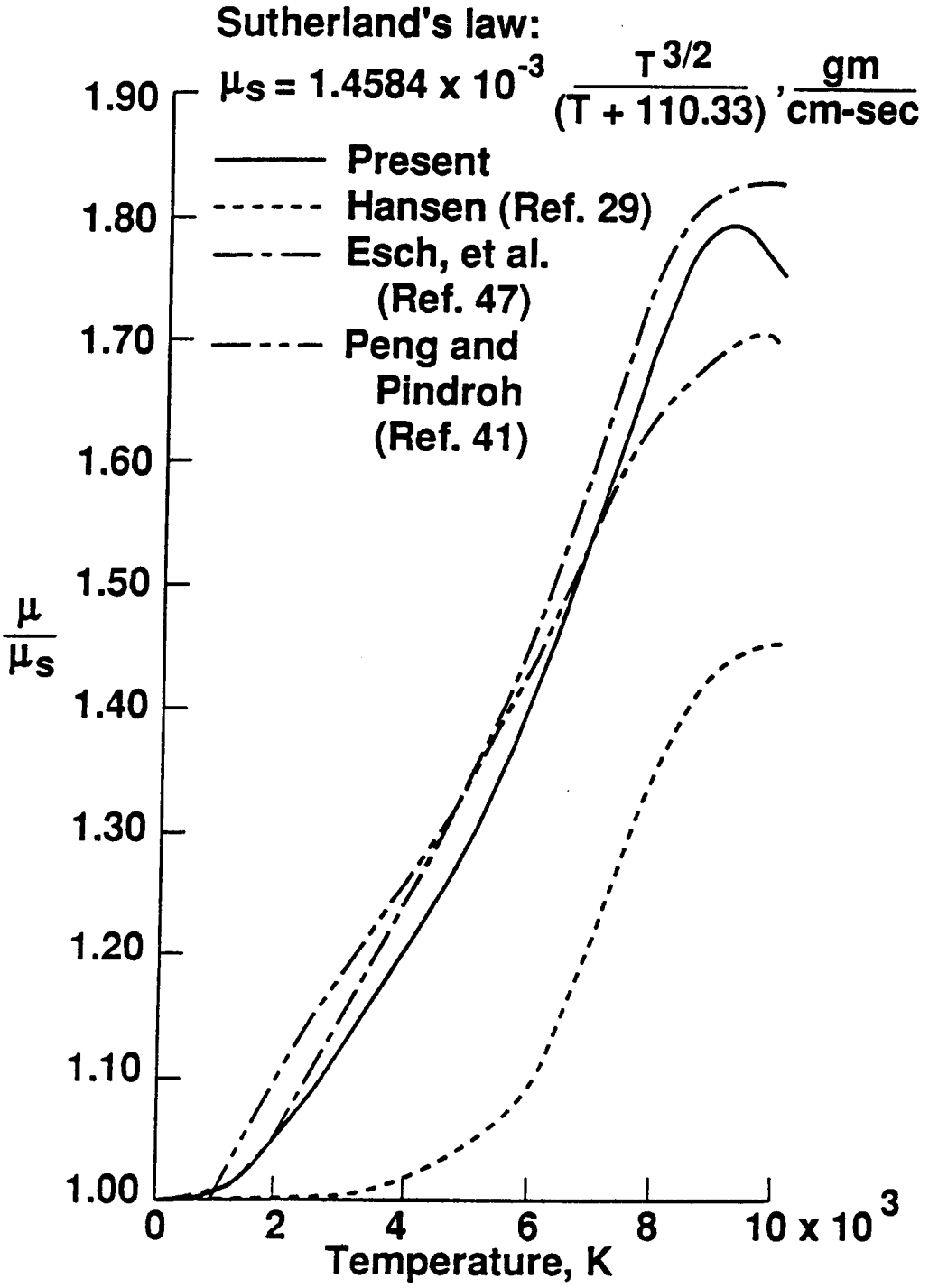

Figure 6. Comparison of the viscosity of equilibrium air at 1 atmosphere.

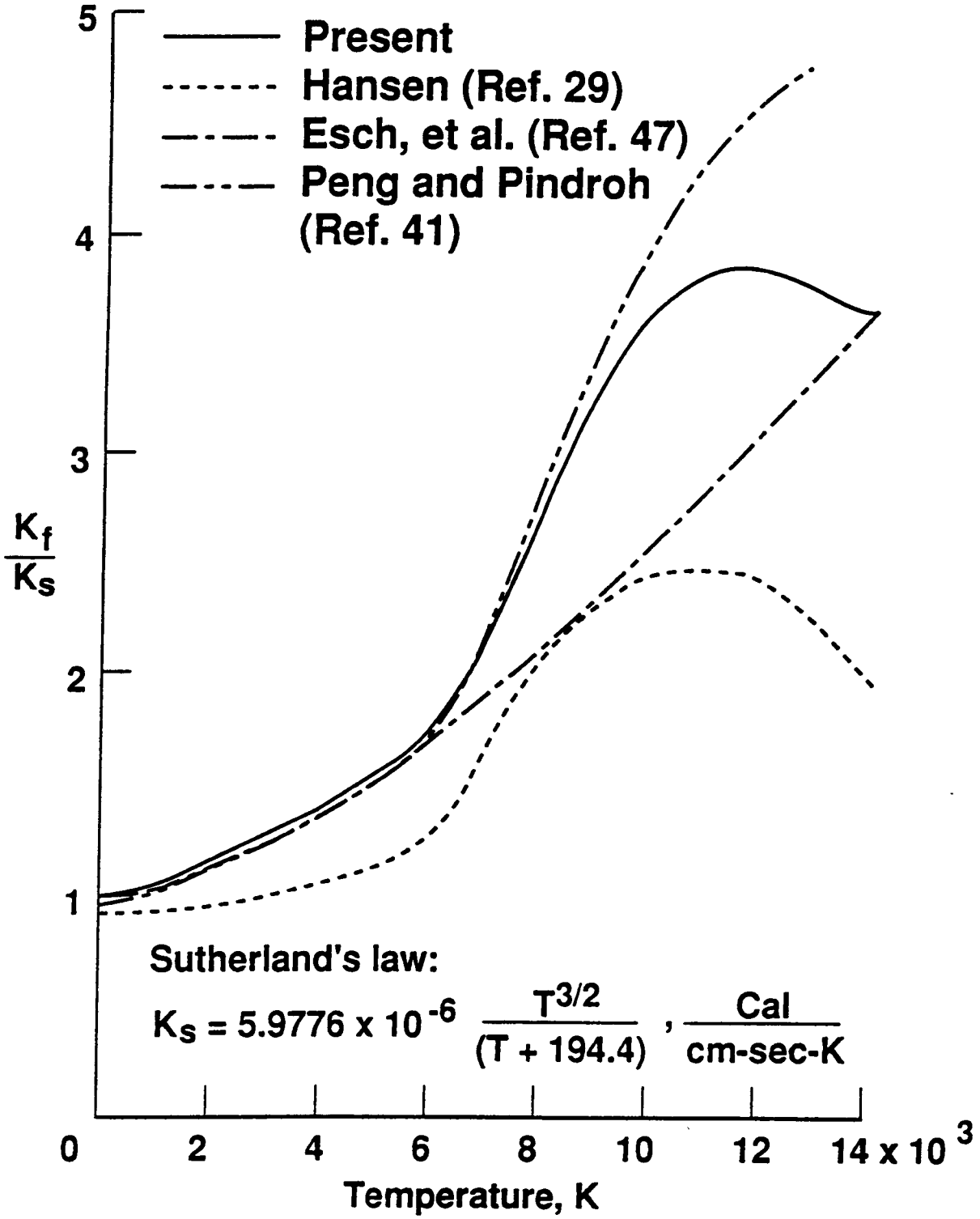

Figure 7. Comparison of the frozen thermal conductivity of equilibrium air at 1 atmosphere.

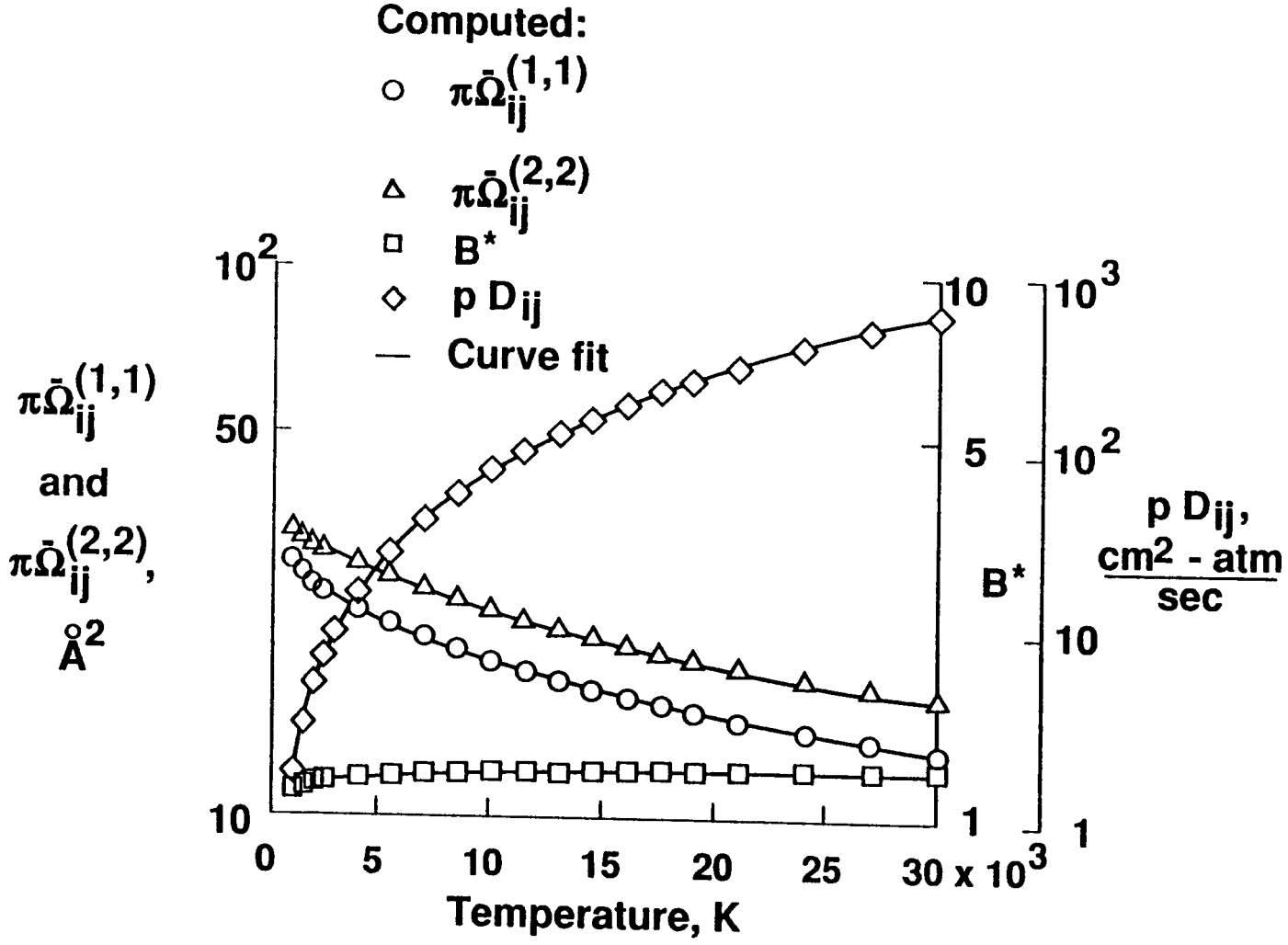

(a) Neutral-neutral molecular interaction: $O_2 \leftrightarrow O_2$

Figure 8. Curve fit to the computed values of collision integrals, collision integral ratio, and binary diffusion coefficient obtained by employing the data of Yos (ref. 32).
(a) Neutral-neutral molecular interaction: $O_2 \leftrightarrow O_2$

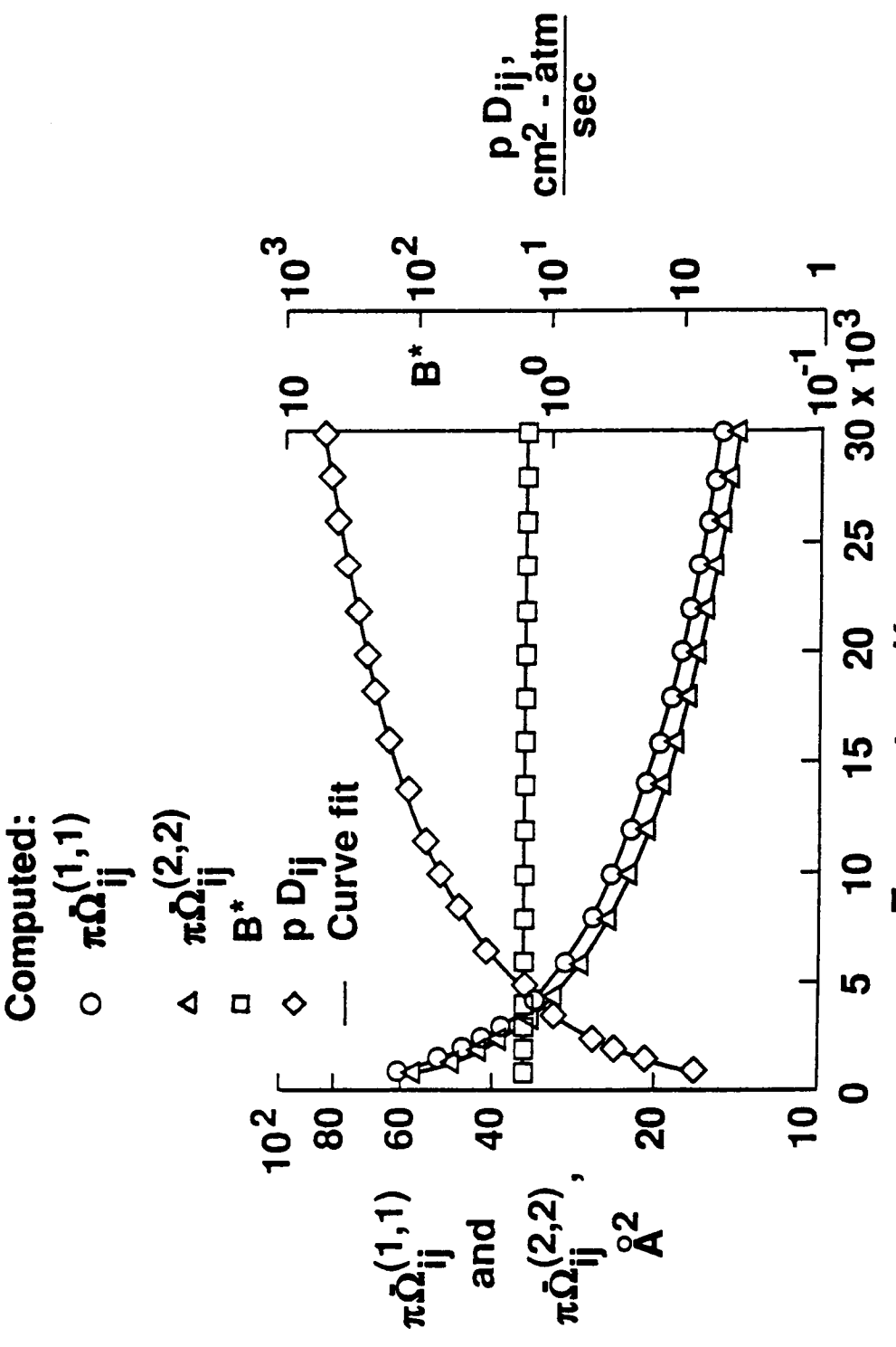

(b) Ion-neutral molecular interaction: $NO^+ \leftrightarrow O_2$

Figure 8. Continued.

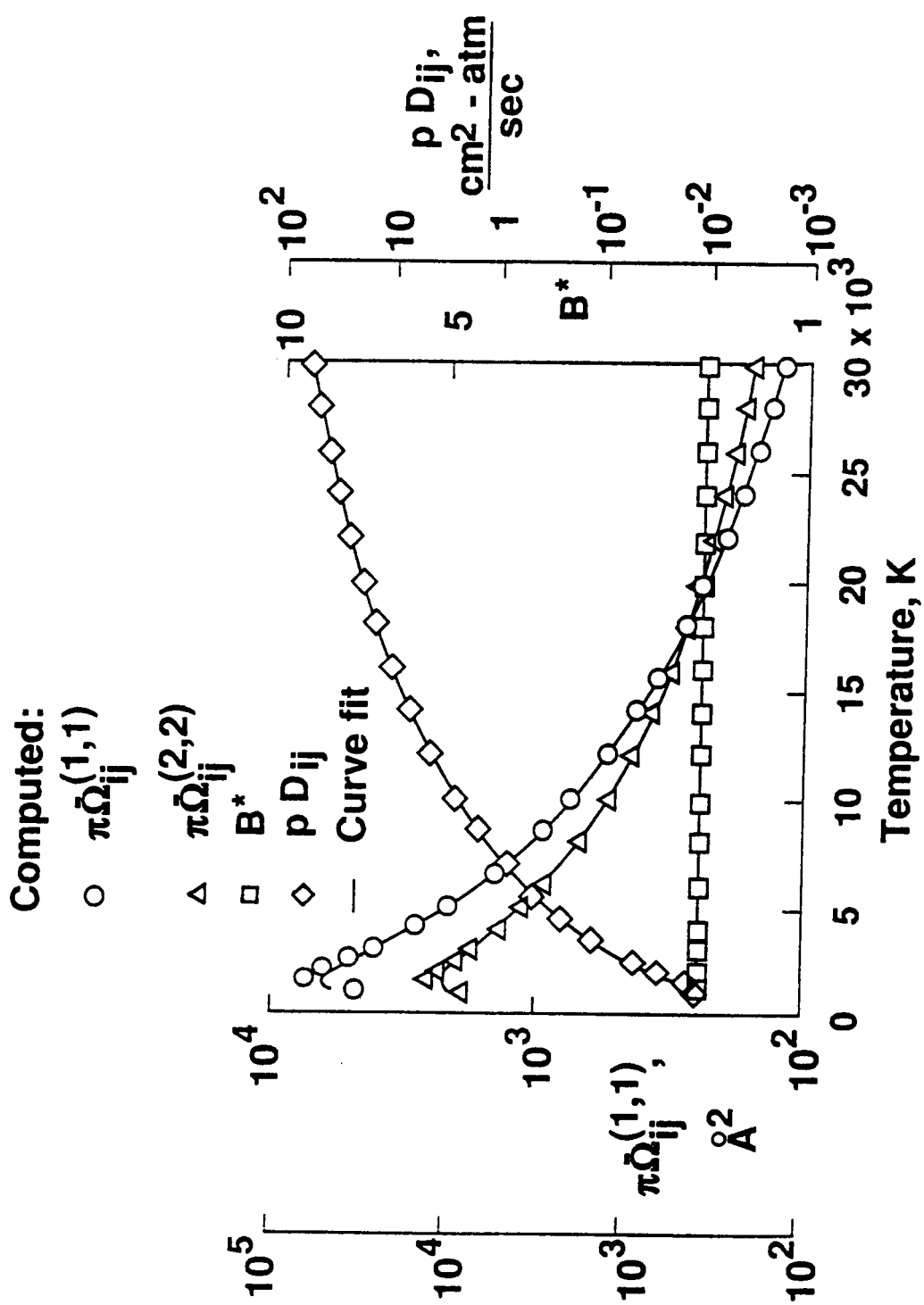

(c) Ion-ion molecular interaction: $NO^+ \leftrightarrow NO^+$

Figure 8. Continued.

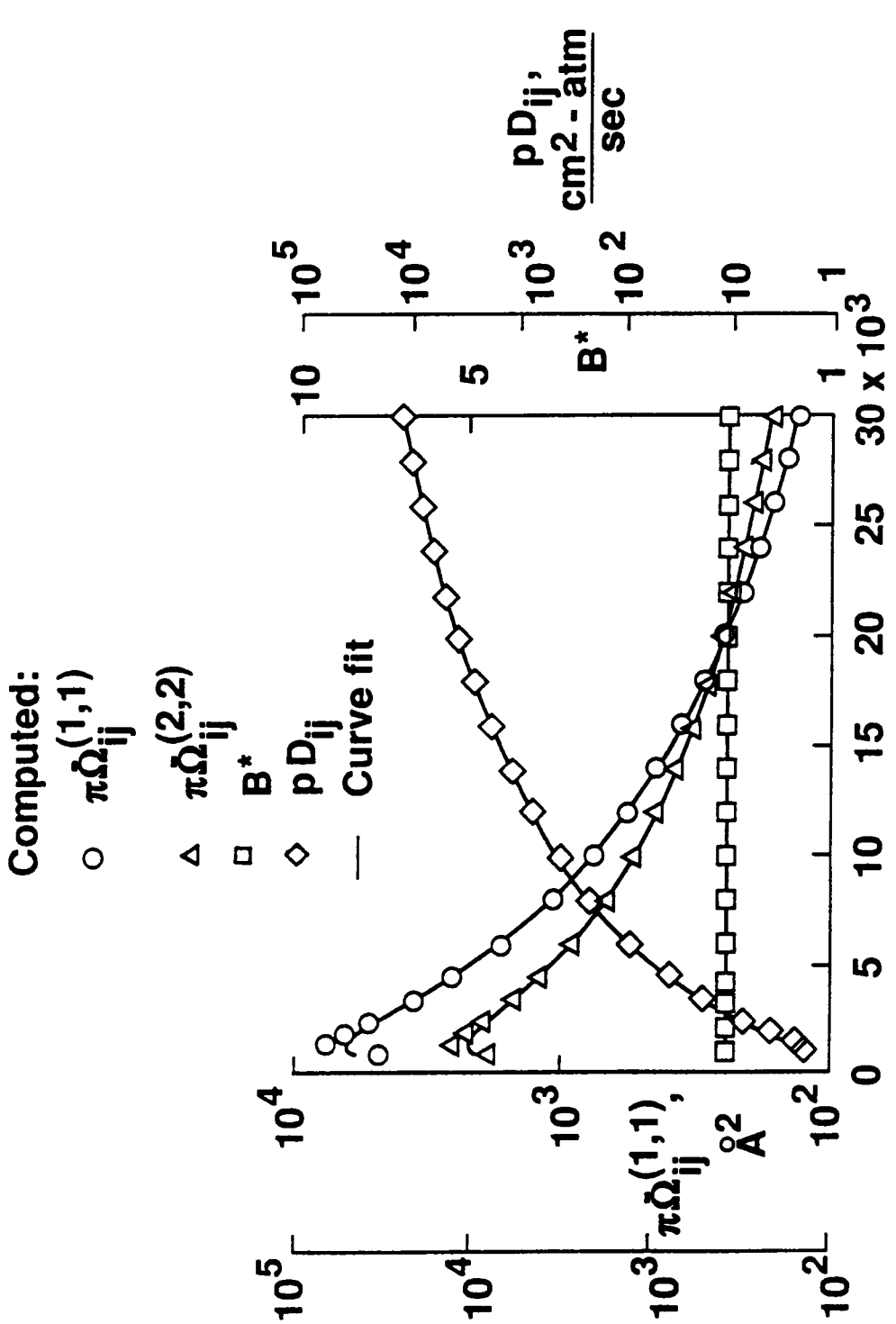

(d) Electron-ionized-molecule interaction: $NO^+ \leftrightarrow e^-$

Figure 8. Continued.

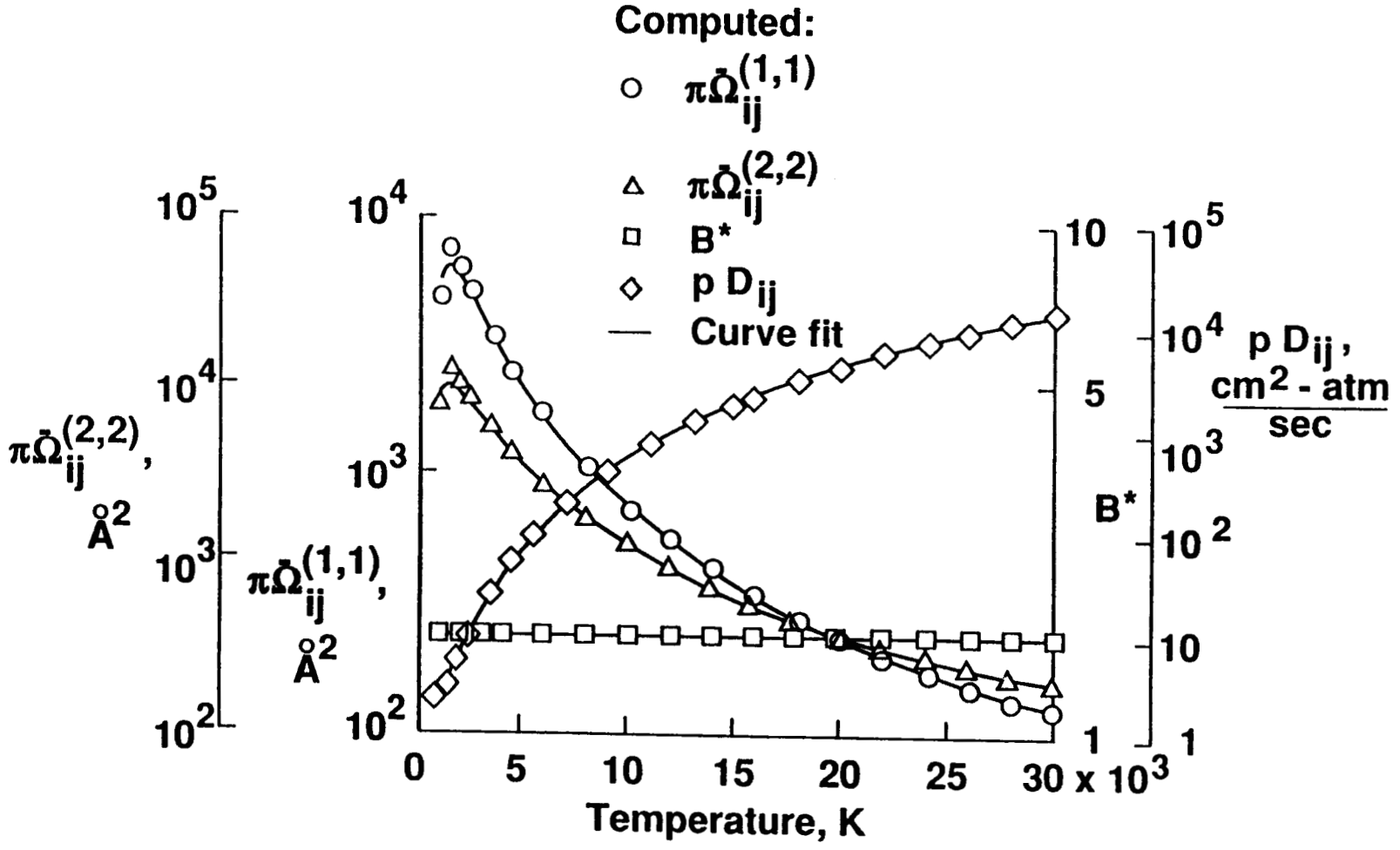

(e) Electron-electron interaction: $e^- \leftrightarrow e^-$

Figure 8. Concluded.

NASA National Aeronautics and Space Administration

Report Documentation Page

1. Report No.	2. Government Accession No.	3. Recipient's Catalog No.
NASA TM-101528		

4. Title and Subtitle
A Review of Reaction Rates and Thermodynamic and Transport Properties for the 11-Species Air Model for Chemical and Thermal Nonequilibrium Calculations to 30000 K

5. Report Date
February 1989

6. Performing Organization Code

7. Author(s)
Roop N. Gupta
Jerrold M. Yos
Richard A. Thompson

8. Performing Organization Report No.

10. Work Unit No.
763-01-31-19

9. Performing Organization Name and Address
NASA Langley Research Center
Hampton, Virginia 23665-5225

11. Contract or Grant No.

13. Type of Report and Period Covered
Technical Memorandum

12. Sponsoring Agency Name and Address
National Aeronautics and Space Administration
Washington, DC 20546-0001

14. Sponsoring Agency Code

15. Supplementary Notes
Roop N. Gupta: Scientific Research and Technology, Inc., Hampton, Virginia
Jerrold M. Yos: AVCO Systems, Wilmington, Massachusetts
Richard A. Thompson: Langley Research Center, Hampton, Virginia

16. Abstract

Reaction rate coefficients and thermodynamic and transport properties are provided for the 11-species air model which can be used for analyzing flows in chemical and thermal nonequilibrium. Such flows will likely occur around currently planned and future hypersonic vehicles. Guidelines for determining the state of the surrounding environment are provided. Approximate and more exact formulas are provided for computing the properties of partially ionized air mixtures in such environments.

17. Key Words (Suggested by Author(s))	18. Distribution Statement
Hypersonic nonequilibrium flow Chemical reaction rates Thermodynamic and transport properties 11-species air model	Unclassified-Unlimited Subject Category 34

19. Security Classif. (of this report)	20. Security Classif. (of this page)	21. No. of pages	22. Price
Unclassified	Unclassified	68	A04